THE BELL SYSTEM TECHNICAL JOURNAL
Vol. 51, No. 1, January, 1972
Printed in U.S.A.

Waiting Time Jitter

By D. L. DUTTWEILER

(Manuscript received July 15, 1971)

Waiting time jitter is a low-frequency phase jitter introduced whenever asynchronous digital signals are synchronized for multiplexing by pulse stuffing. It contains arbitrarily low frequency components and cannot be completely removed from the demultiplexed signals.

In this paper the spectrum of waiting time jitter is derived, and supporting experimentally recorded waiting time jitter spectra are presented.

A question of much engineering interest is at what rate waiting time jitter accumulates in a chain of multiplexer-demultiplexer pairs. A calculation based on the theoretical waiting time jitter spectrum shows that under reasonable conditions the rate at which the rms amplitude of the accumulated waiting time jitter grows is no greater than the square root of the number of multiplexer-demultiplexer pairs. Experimental data consistent with this upper bound are given.

I. INTRODUCTION

When a number of lower speed digital signals are to be time division multiplexed to form a higher speed signal, it is necessary that the lower speed signals all be synchronous. If the sources of these signals are remote, this synchronization will be difficult to achieve.

One way of achieving it is to distribute timing information from a master clock to the local clocks at the sources of the lower speed digital signals. In many situations, however, using a master clock and synchronizing the entire digital communication network is either not possible or not economically desirable.

An alternative method of achieving synchronization is to use pulse stuffing synchronization.[1,2] The pulse stuffing synchronization scheme is reviewed in the next section. Basically, the idea is to bring the symbol rates of each of the incoming lines up to some common rate just before multiplexing by inserting dummy pulses. After demultiplexing, the dummy pulses are removed and each of the signals retimed to smooth out the gaps.

The retiming can never be done perfectly. There is always a phase jitter present on the demultiplexed signals. In Sections III and IV the spectrum of this degrading jitter is derived. Its accumulation in chains of multiplexer-demultiplexer pairs is studied in Section VI.

II. PULSE STUFFING SYNCHRONIZATION

It is convenient to review pulse stuffing synchronization by describing the operation of a particular system. Since our experimental data were taken on the M12 multiplex, we have chosen this system to describe.[3] The reader should have no difficulty generalizing to other systems. The few details of the operation of the M12 that are essential for our discussion will be reviewed where necessary.

The M12 is designed to multiplex four asynchronous DS-1 digital signals (nominally 1.544 Mb/s) into a DS-2 bit stream (nominally 6.312 Mb/s).[4] For each of the four DS-1 digital data streams there is associated circuitry in the M12 designed to insert dummy pulses and bring its symbol rate up to a common one.

A block diagram of one of these synchronizers is shown in Figure 1.

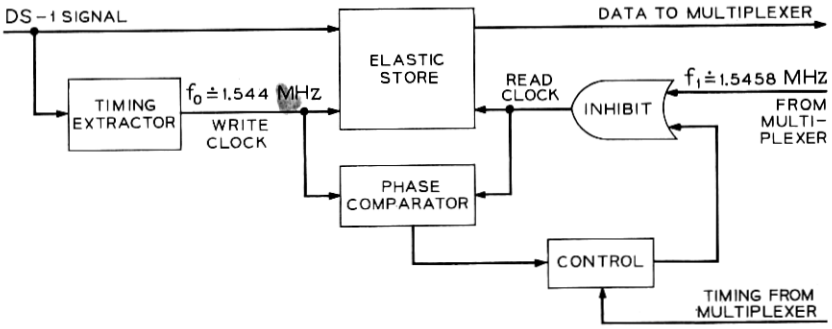

Fig. 1—A block diagram of one of the four synchronizers in an M12.

The data is written into the elastic store under the influence of the write clock, and read out under the influence of the read clock. The write clock is derived from the DS-1 signal. Its frequency (nominally 1.544 MHz) will be denoted by f_0 and its period, by $t_0 = 1/f_0$.*

The clocking signal at the input to the inhibit gate is derived from

* In making these definitions it is being tacitly assumed that there is no jitter on the write clock. This assumption will not always be reasonable since there may be jitter on the DS-1 signal from which it is derived. The effects of this jitter are studied in Section V.

a local clock. It is identical except for constant phase offsets with the corresponding clocking signals in the other three synchronizers. Thus, the data read out of the four synchronizers can be multiplexed by interleaving with no difficulty.

The pulses on the clocking signal at the input to the inhibit gate are normally separated by four DS-2 time slots. Every twelfth pulse is separated from its successor by five DS-2 time slots to allow framing and control pulses to be inserted onto the DS-2 signal. The average frequency of this clocking signal will be denoted by f_1 and its average period by $t_1 = 1/f_1$. Nominally,

$$f_1 = (12/49) \cdot 6.312 = 1.5458 \text{ MHz}.$$

For the remainder of this paper, the jitter on this clocking signal will be neglected, and it will be approximated as an unjittered clocking signal with frequency f_1.*

By design the frequency f_1 is greater than f_0. If all the pulses at the input to the inhibit gate were allowed to pass through, the read clock would eventually overtake the write clock. Since it is necessary to write before reading, some pulses must be inhibited.

The inhibiting of pulses is done by the phase comparator and associated control circuitry. The output of the phase comparator, $\phi_S(t)$, is the phase difference between the read and write clocks (or, equivalently, the jitter on the output data stream of the synchronizer). The control circuitry monitors $\phi_S(t)$ and as soon as possible after $\phi_S(t)$ crosses some predetermined threshold Λ inhibits a clocking pulse, or, as it is more commonly phrased, stuffs a (data) pulse.

A typical graph of $\phi_S(t)$ is shown in Figure 2. By convention $\phi_S(t)$ is defined as positive if the read clock precedes the write clock. This seemingly backwards definition gives $\phi_S(t)$ positive slope and negative jumps as seems to be traditional.[5,6] Since the write clock must always precede the read clock, the threshold Λ must be set so that $\phi_S(t)$ is always negative.

The positive slope of $\phi_S(t)$ at nonjump times reflects the fact that in the absence of inhibit pulses the read clock is gradually overtaking the write clock. Whenever a pulse is stuffed, $\phi_S(t)$ drops by one slot (by definition one slot equals t_1 seconds). Stuffing does not occur as soon as $\phi_S(t)$ crosses the threshold. It is necessary to wait until a stuffing

* The techniques of Section V could be used to remove this assumption also. It is not particularly interesting to do so, however, since little error results from making it. The jitter being neglected is systematic and of relatively high frequency. It is easily removed at the demultiplexer.

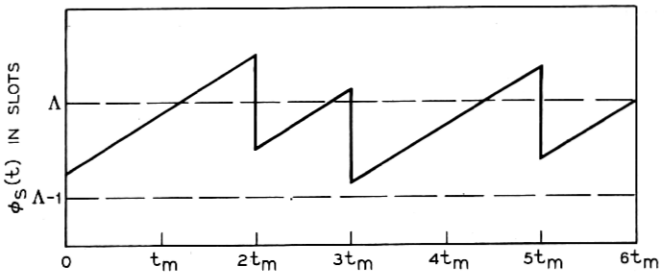

Fig. 2—A typical graph of the output of the phase comparator.

opportunity occurs. These opportunities, which are fixed by M12 format considerations, occur at regular intervals 1176 DS-2 time slots apart. Let t_m denote this interval. Then,

$$t_m = 1176 \cdot (12/49)\ t_1$$
$$= 288\ t_1\ .$$

The maximum possible stuffing rate is $f_m = 1/t_m$. In the M12

$$f_m = 6.312/1176 \text{ MHz}$$
$$= 5.367 \text{ kHz}.$$

The actual average rate at which pulses are being stuffed is $f_s = f_1 - f_0$. The stuffing ratio

$$\rho = f_s/f_m\ ,$$

which must be between 0 and 1, is a critical parameter. Nominally, in the M12

$$\rho = f_s/f_m = (f_1 - f_0)/f_m$$
$$= \frac{(12/49)\cdot 6.312 - 1.544}{6.312/1176}$$
$$= 0.3346,$$

or slightly more than 1/3.

It will be convenient for the remainder of this paper to measure time in stuffing opportunities and frequency in cycles per stuffing opportunity. All numerical values for times and frequencies given from here on are to be assumed to have these units unless other units are explicitly stated. Conversion to seconds and Hertz is easy through

the relations

$$1 \text{ stuffing opportunity} = 0.186 \text{ ms}$$

and

$$1 \text{ cycle per stuffing opportunity} = 5.367 \text{ kHz}.$$

It has been traditional to consider $\phi_S(t)$ as being the sum of two jitter waveforms—the first being stuffing jitter and the second waiting time jitter. Stuffing jitter is defined as the jitter that would be present if stuffing could occur on demand, and waiting time jitter is usually defined as the low-frequency jitter present in $\phi_S(t)$ because in actuality there is a "waiting time" between stuff demand and stuff execution. Since these definitions are hard to make precise, we shall not attempt to make any such distinctions and shall merely call $\phi_S(t)$ the waiting time jitter waveform.

After each of the four DS-1 signals is synchronized, it is multiplexed with the other three, transmitted over an appropriate facility and demultiplexed by an M12. Stuffed pulses on each of the lines are removed in an associated desynchronizer.

A block diagram of a desynchronizer is shown in Figure 3. Information telling the demultiplexer where stuffs have been made is carried on the DS-2 signal along with the data. Thus, it is possible for the write clock in the desynchonizer to exactly duplicate the read clock in the synchronizer. It has gaps where stuffs were made.

The read clock on the elastic store in the desynchronizer is obtained from a voltage controlled oscillator (VCO). The output of the phase comparator, which is proportional to the phase difference between the read and write clocks, is filtered and fed back to the VCO in such a way as to keep the read clock from overtaking or falling too far behind the write clock.

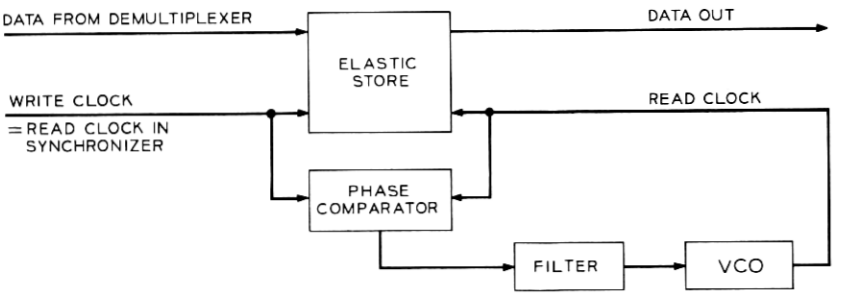

Fig. 3—A block diagram of one of the four desynchronizers in an M12.

The desynchronizer acts as a phase-locked loop and smooths the gaps created by stuffing pulses. Ideally, the output of the desynchronizer would be identical with the input to the synchronizer. Unfortunately, all phase-locked loops have a low-pass nature and some low-frequency jitter degrades the output.

Let $\phi_D(t)$ denote this jitter. Then

$$\phi_D(t) = h(t)*\phi_S(t),$$

where $h(t)$ is the overall transfer function of the phase-locked loop in the desynchronizer and * denotes convolution. In the M12 $h(t)$ falls off at 12 dB per octave after cutoff at about 0.12 cycle per stuffing opportunity (644 Hz).*

Often $\phi_S(t)$ and $\phi_D(t)$ are both called waiting time jitter (distinguishable only by context). To avoid any confusion, we shall only call $\phi_S(t)$ waiting time jitter and shall always call $\phi_D(t)$ filtered waiting time jitter.

Because of the low-pass nature of $h(t)$, the low-frequency components of waiting time jitter are present in filtered waiting time jitter and degrade the demultiplexed signal. It is not difficult to demonstrate that it is quite possible for $\phi_S(t)$ to contain significant low-frequency power. In Figure 4a, $\phi_S(t)$ is drawn assuming $\rho = 1/2$. The lowest frequency component in this waveform is at the relatively high frequency of 1/2 cycle per stuffing opportunity. But, it is unrealistic to assume $\rho = 1/2$ exactly. Figures 4b and 4c show $\phi_S(t)$ for ρ slightly greater than 1/2 and ρ slightly less than 1/2. In both cases there is a strong low-frequency envelope. In general, whenever ρ is close to a simple rational number (a rational number with a small denominator), but not exactly equal to it, $\phi_S(t)$ will have appreciable low-frequency power.

This idea is developed in papers by Kozuka[5] and Matsuura, Kozuka, and Yuki[6]. Formulas are given for the peak-to-peak amplitude of the low-frequency envelope present on the waveform $\phi_S(t)$ when ρ is close to, but not exactly equal to, a simple rational number. Questions arise, however, as to how close is close enough and how the trade off between approximation accuracy and simpler rational numbers is to be made (for example, should 0.45^+ be considered close to 1/2 or to 9/20?).

An alternate approach is to calculate the power spectrum of waiting time jitter as we do in the next section.

---

* The M12 has been recently redesigned and now has a lower cutoff frequency.

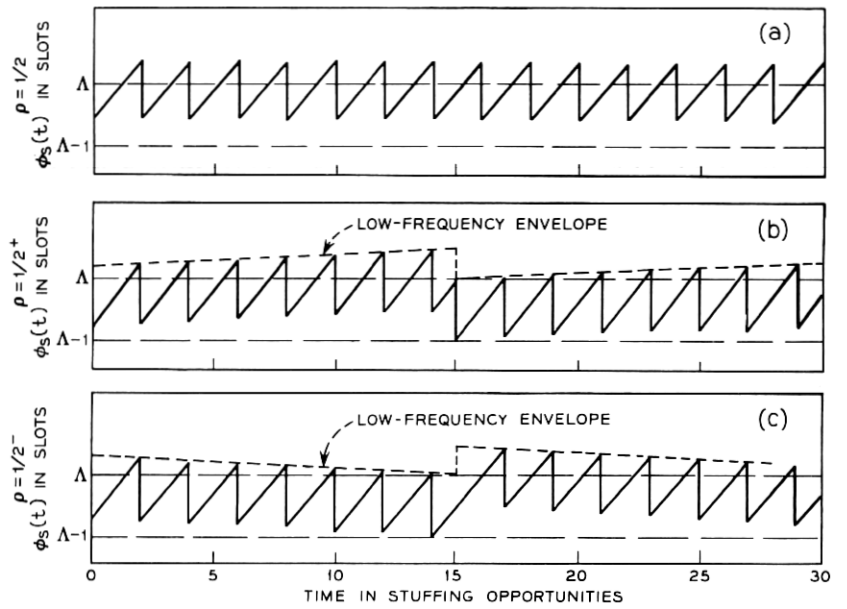

Fig. 4—In the upper portion of this figure ρ equals 1/2 exactly, and there are no low-frequency components in $\Phi_S(t)$. In the other portions of this figure ρ is close but not exactly equal to 1/2, and there are strong low-frequency components.

III. THE SPECTRUM OF WAITING TIME JITTER

3.1 *Theoretical*

In Appendix A the power spectrum $S_s(f)$ of $\phi_s(t)$ is calculated. Briefly, the procedure used is to (*i*) find an equation describing waiting time jitter waveforms, (*ii*) introduce initial condition random variables into this equation in such a way that a stationary ensemble of waiting time jitter waveforms is defined, (*iii*) compute the covariance of the waiting time jitter random process, and (*iv*) Fourier transform this covariance to obtain the power spectrum $S_s(f)$.

It is possible to find the power spectrum of waiting time jitter without using random process theory. A procedure similar to one used by Iwerson[7] to find the spectrum of quantizing noise in a delta modulator with unequal positive and negative step sizes could be used. (The similarity of the underlying mathematics in these two at first seemingly unrelated problems is remarkable.) Our method of finding the spectrum (that is, via random processes) does not require any approximations. The method used by Iwerson requires approximating pulses by delta

functions. This approximation is unimportant for his problem, but of more consequence in the waiting time jitter problem. A further advantage of proceeding via random process theory is that the arguments needed are somewhat simpler and more concise, especially those that are given in Appendix B of this paper (corresponding with those in Appendix D of the paper by Iwerson).

The result of Appendix A is (remember, frequency is being measured in cycles per stuffing opportunity)

$$S_S(f) = \operatorname{sinc}^2 f \cdot Q(f) + \sum_{n=1}^{\infty} \left(\frac{\rho}{2\pi n}\right)^2 (\delta(f - n) + \delta(f + n)), \tag{1}$$

where

$$\operatorname{sinc} f = \frac{\sin \pi f}{\pi f},$$

$$Q(f) = \sum_{n=1}^{\infty} \left(\frac{1}{2\pi n}\right)^2 (\operatorname{rep} \delta(f - \rho n) + \operatorname{rep} \delta(f + \rho n)), \tag{2}$$

$$\operatorname{rep} X(f) = \sum_{k=-\infty}^{\infty} X(f - k) \quad \text{for any function } X(f),$$

and $\delta(\cdot)$ is the Dirac delta function. It is convenient to define

$$S_{S,A}(f) = \operatorname{sinc}^2 f \cdot Q(f) \tag{3}$$

and

$$S_{S,B}(f) = \sum_{n=1}^{\infty} \left(\frac{\rho}{2\pi n}\right)^2 (\delta(f - n) + \delta(f - n)). \tag{4}$$

With this notation

$$S_S(f) = S_{S,A}(f) + S_{S,B}(f).$$

Graphs of $\operatorname{sinc}^2 f$, $Q(f)$, and $S_{S,B}(f)$ are given in Figure 5. Only the lines associated with the first, second, and third terms of the defining sum for $Q(f)$ are shown in the graph of $Q(f)$. The lines labeled 1^- are lines introduced by

$$\left(\frac{1}{2\pi \cdot 1}\right)^2 \operatorname{rep} \delta(f - \rho \cdot 1).$$

Lines labeled 1^+ are lines introduced by

$$\left(\frac{1}{2\pi \cdot 1}\right)^2 \operatorname{rep} \delta(f + \rho \cdot 1).$$

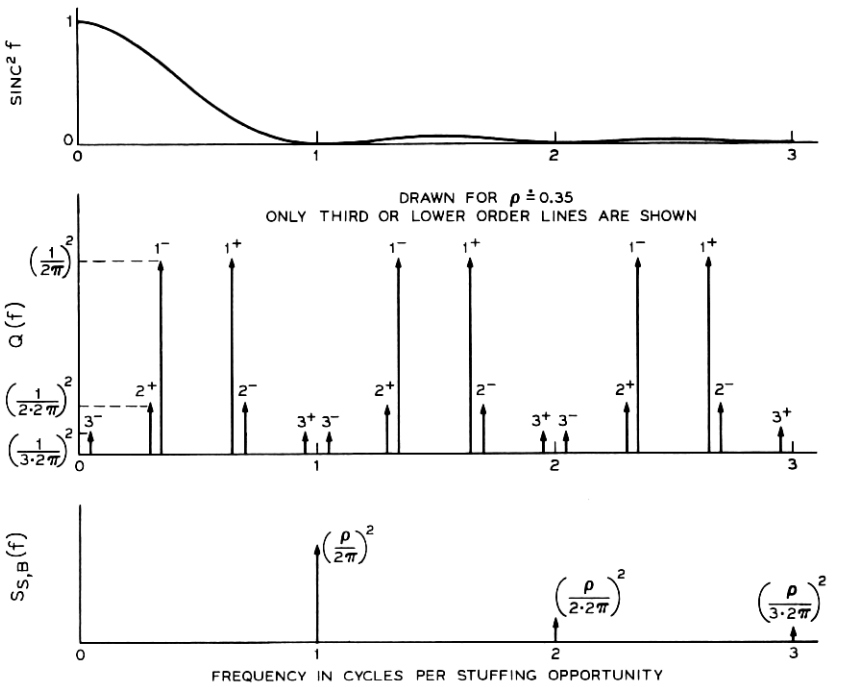

Fig. 5—The components of the spectrum of waiting time jitter.

In general, n^--lines and n^+-lines are lines introduced by

$$\left(\frac{1}{2\pi n}\right)^2 \text{ rep } \delta(f - \rho n)$$

and

$$\left(\frac{1}{2\pi n}\right)^2 \text{ rep } \delta(f + \rho n)$$

respectively. This notational scheme is similar to the one used by Iwerson.

The interesting information about the spectrum $S_S(f)$ is carried by $Q(f)$. $S_{S,B}(f)$ contains only relatively high-frequency components. The function $\text{sinc}^2 f$ is just an envelope. The low-frequency content of $S_S(f)$ is determined by ρ through $Q(f)$.

If ρ is irrational, none of the spectral lines will coincide. When ρ is rational, the spectral lines do eventually coincide and it is possible

to replace the infinite sum in the defining equation for $Q(f)$ by a finite sum. Iwerson shows that if $\rho = p/q$ where p and q are relatively prime,

$$Q(f) = \frac{1}{4q^2} \sum_{n=1}^{q-1} \csc^2\left(\frac{n}{q}\pi\right) \text{rep } \delta\left(f - \frac{pn}{q}\right) + \frac{1}{12q^2} \text{rep } \delta(f). \quad (5)$$

3.2 *Experimental*

The spectra of waiting time jitter waveforms produced by an M12 were recorded for a number of stuffing ratios. Three representative spectra are shown in Figures 6, 7, and 8. The stuffing ratios in these three figures are respectively 0.186, 0.372, and 0.333. The stuffing ratio was varied by varying the DS-1 symbol rate.

The vertical dB scale on the graphs is only approximate. In addition, no attempt was made to have 0 dB correspond to any particular amount of jitter power, and therefore, readings taken from it are only relative.

In Figures 6 and 7 the stuffing ratio is not close to any simple rational number and the spectral lines are all distinct. To record Figure 8, the stuffing ratio was set as close as possible to 1/3. The expected coincidence of lines is quite apparent.

The weak line at about 0.08 cycle per stuffing opportunity in Figure 8 is not present in the theoretical spectrum. Its origin can be traced to an improper (only in the sense that it deviates from the usual model) functioning of the synchronizer in the M12. This improper functioning,

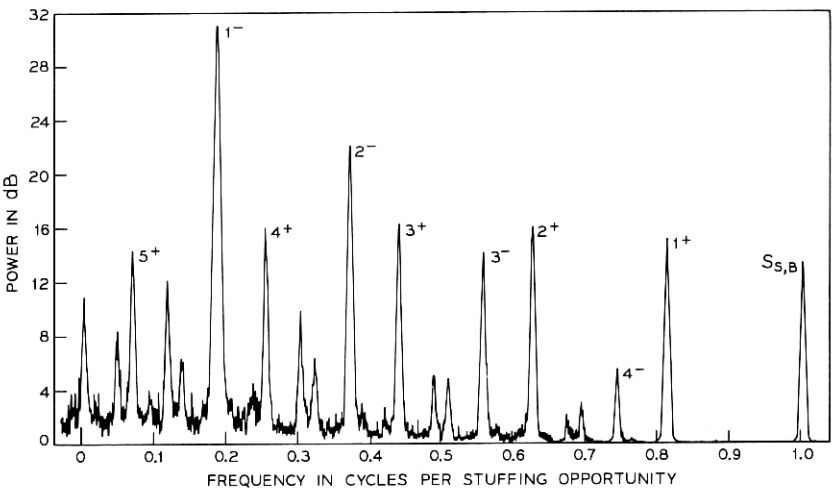

Fig. 6—An experimental waiting time jitter spectrum with $\rho = 0.186$.

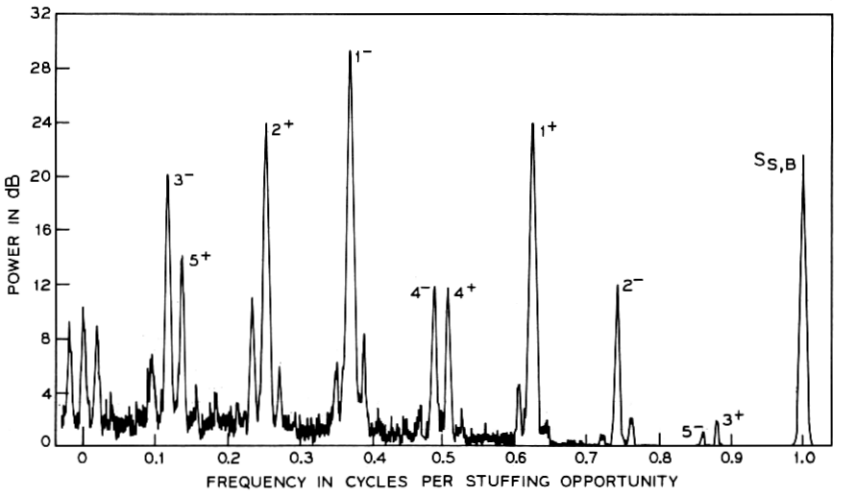

Fig. 7—An experimental waiting time jitter spectrum with $\rho = 0.372$.

termed multiple stuffing, is also apparent when looking at oscilloscope traces of waiting time jitter waveforms. Occasionally stuffs will be made when they quite obviously should not be (for instance, twice in a row with $\rho < 1/2$). The actual M12 used to record the spectra of Figures 6, 7, and 8 was an experimental model having an asynchronous

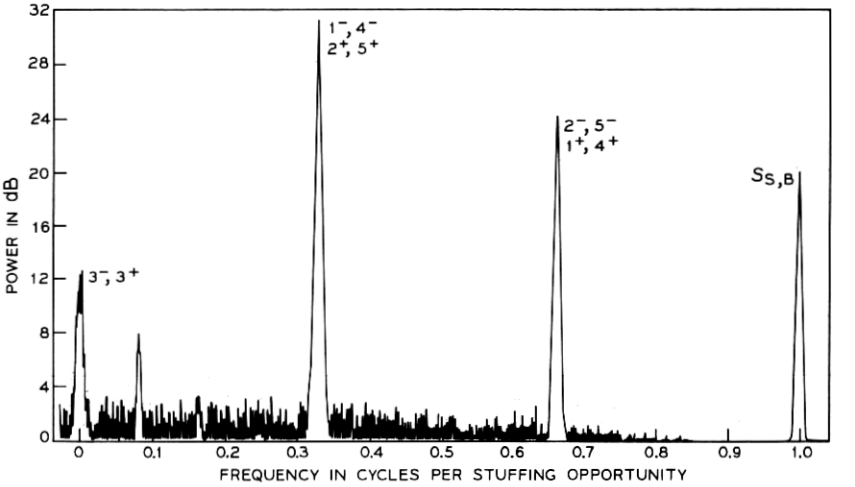

Fig. 8—An experimental waiting time jitter spectrum with $\rho = 0.333$.

delay line[8] elastic store rather than the usual commutator type (see page 617 of Ref. 4). It was used because it exhibited slightly less multiple stuffing.

In Tables I, II, and III the powers of the lines in the experimental and theoretical waiting time jitter spectra are tabulated for the stuffing ratios 0.186, 0.372, and 0.333 respectively. To obtain the theoretical powers listed in Tables I and II, equation (2) for $Q(f)$ was used. The rational stuffing ratio formula (5) for $Q(f)$ was used in computing the theoretical powers listed in Table III.

The entries in the columns headed uncorrected experimental power were simply read off Figures 6, 7, and 8. For ease of comparison corrected experimental powers are also listed. These entries were obtained by multiplying the corresponding uncorrected powers by 0.817 (to correct the vertical scaling) and subtracting 42.0 (to add an absolute reference). The constants 0.817 and 42.0 were chosen by a least squares procedure.

The differences between the theoretical and corrected experimental powers are listed in the last column of Tables I, II, and III. The agreement is to within 0.5 dB except in a few cases where discrepancies are easily explained in terms of the low frequency and small amplitude limitations of the spectrum analyzer.

IV. THE RMS AMPLITUDE OF FILTERED WAITING TIME JITTER

4.1 *Theoretical*

Since

$$\phi_D(t) = h(t)*\phi_S(t),$$

TABLE I—SPECTRAL LINE POWERS FOR $\rho = 0.186$

Line	Normalized Frequency	Power (dB)			
		Theoretical	Experimental Uncorrected	Experimental Corrected	Difference
1^-	0.186	−16.5	31.0	−16.6	−0.1
2^-	0.372	−24.1	22.3	−23.7	0.4
3^-	0.558	−30.5	14.1	−30.4	0.1
4^-	0.744	−38.2	5.6	−37.4	0.8
5^-	0.930	−52.5	—	—	—
1^+	0.814	−29.3	15.2	−29.5	−0.2
2^+	0.628	−28.6	16.1	−28.8	−0.2
3^+	0.442	−28.5	16.3	−28.6	−0.1
4^+	0.256	−29.0	15.8	−29.0	0.0
5^+	0.070	−30.0	14.3	−30.3	−0.3
$S_{S,B}$	1.000	−30.6	13.5	−30.9	−0.3

TABLE II—SPECTRAL LINE POWERS FOR $\rho = 0.372$

Line	Normalized Frequency	Power (dB)			
		Theoretical	Experimental Uncorrected	Experimental Corrected	Difference
1^-	0.372	−18.0	29.4	−17.9	0.1
2^-	0.744	−32.2	11.8	−32.3	−0.1
3^-	0.116	−25.7	20.1	−25.5	0.2
4^-	0.488	−31.8	11.8	−32.3	−0.5
5^-	0.860	−46.0	1.2	−41.0	5.0
1^+	0.628	−22.6	24.0	−22.4	0.2
2^+	0.256	−22.9	23.8	−22.5	0.4
3^+	0.884	−43.3	2.0	−40.3	3.0
4^+	0.512	−32.1	11.6	−32.5	−0.4
5^+	0.140	−30.2	14.0	−30.5	−0.3
$S_{S,B}$	1.000	−24.6	21.3	−24.6	0.0

the spectrum $S_D(f)$ of filtered waiting time jitter is given by

$$S_D(f) = |H(f)|^2 S_S(f)$$

where $H(f)$ is the Fourier transform of $h(t)$, that is,

$$H(f) = \mathfrak{F}\{h(t)\} = \int_{-\infty}^{\infty} h(t)e^{-j2\pi ft}\,dt.$$

Only the low frequency components of $S_S(f)$ will not be significantly attenuated by $|H(f)|^2$.

The power $P_D(\rho)$ in $\phi_D(t)$ (that is, the rms amplitude squared of $\phi_D(t)$) is given by

$$\begin{aligned} P_D(\rho) &= \int_{-\infty}^{\infty} S_D(f)\,df \\ &= \int_{-\infty}^{\infty} |H(f)|^2 S_S(f)\,df \\ &= \int_{-\infty}^{\infty} |H(f)|^2 S_{S,A}(f)\,df + \int_{-\infty}^{\infty} |H(f)|^2 S_{S,B}(f)\,df \\ &\triangleq P_{D,A}(\rho) + P_{D,B}(\rho). \end{aligned}$$

Typically, $h(t)$ cuts off at frequencies much smaller than 1 cycle per stuffing opportunity where the lowest frequency spectral line in $S_{S,B}(f)$ is located, and, therefore, $P_{D,B}(\rho)$ is quite small in comparison to $P_{D,A}(\rho)$. Since $P_{D,A}(\rho)$ is symmetric about 1/2 (that is, $P_{D,A}(\rho) = P_{D,A}(1-\rho)$), it is to be expected that $P_D(\rho)$ will be essentially symmetric also.

TABLE III—SPECTRAL LINE POWERS FOR $\rho = 0.333$

Line	Normalized Frequency	Power (dB)			
		Theoretical	Experimental Uncorrected	Experimental Corrected	Difference
$1^-, 2^+, 4^-, 5^+, \cdots$	0.333	−16.0	31.4	−16.3	− 0.3
$1^+, 2^-, 4^+, 5^-, \cdots$	0.667	−22.0	24.2	−22.2	− 0.2
$3^-, 3^+, 6^-, 6^+, \cdots$	0.000	−20.3	12.6	−31.7	−11.4
$S_{S,B}$	1.000	−25.5	20.2	−25.5	0.0

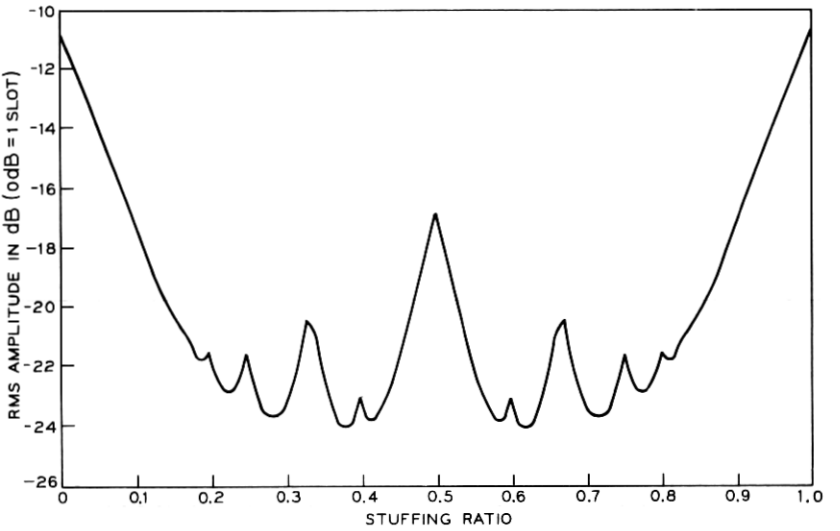

Fig. 9—A theoretical graph of the rms amplitude of filtered waiting time jitter as a function of ρ with $H(f)$ assumed to have a double pole at 0.12 cycle per stuffing opportunity.

A computer program was written to plot $P_D(\rho)$ for various filter transfer functions $H(f)$. Two sample graphs appear in Figures 9 and 10. The assumed transfer functions were respectively

$$H(f) = \left(\frac{0.12}{jf + 0.12}\right)^2$$

and

$$H(f) = \left(\frac{0.06}{jf + 0.06}\right)^2.$$

The first transfer function is a good approximation to that of the filter in the M12*. The cutoff frequency of the second transfer function is 1/2 that of the first. In both graphs the predicted symmetry is quite apparent as are the expected peaks at rational stuffing ratios. The peaking is more pronounced with the sharper filter.

For both filters there appears to be significant benefit to be gained by choosing ρ intelligently. Actually, as will be discussed more fully in Subsection 5.2, this conclusion is misleading because the effect of jitter on the input DS-1 signal has not been considered.

* As noted in a previous footnote, the phase-locked loop in the M12 has been recently redesigned and now has a lower cutoff.

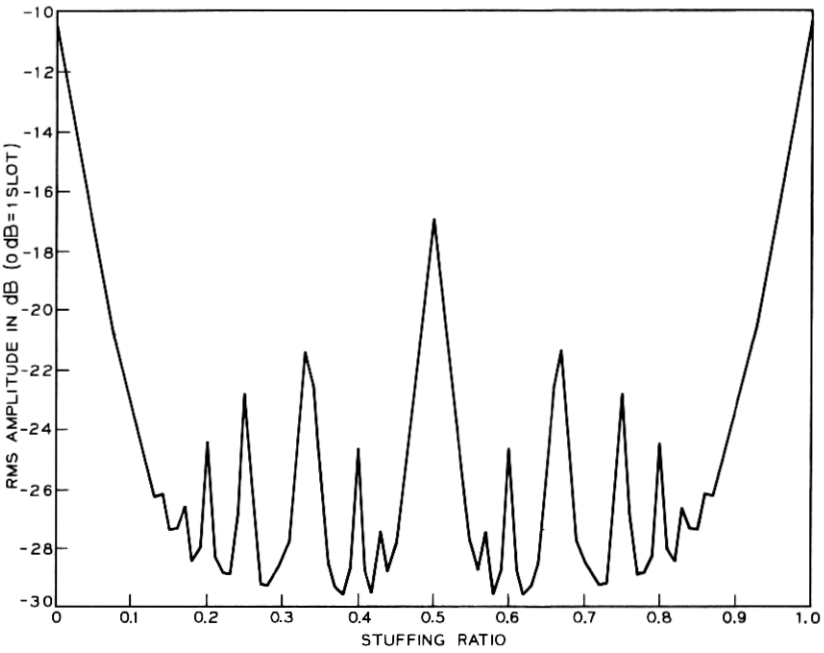

Fig. 10—A theoretical graph of the rms amplitude of filtered waiting time jitter as a function of ρ with $H(f)$ assumed to have a double pole at 0.06 cycle per stuffing opportunity.

4.2 *Experimental*

An experimental recording of $P_D(\rho)$ versus ρ for $\rho \in [0, 1]$ appears in Figure 11. As in the experimental spectra of Figures 6, 7, and 8 the dB scale is only approximate and relative. With this fact taken into account, the agreement with Figure 9 is good.

The vertical lines at the tops of the peaks are caused by the low-frequency cutoff of the true rms voltmeter used in making Figure 11. The unit used cutoff at 10^{-4} cycle per stuffing opportunity (0.5 Hz).

V. INPUT JITTER

5.1 *Generalized Spectrum*

It is possible to generalize the spectrum derivation of Appendix A to allow for jitter already present on the signal at the input to the synchronizer. This jitter will indeed usually be present. If the signal at the input to the synchronizer is coming from a moderately sized T1 line, it will be degraded by significant repeater jitter.[9-11] In addition,

it will be degraded by filtered waiting time jitter if it has already passed through a syndes (synchronizer-desynchronizer pair).

Let $\phi_I(t)$ denote the jitter on the signal at the input to the synchronizer and $\phi_S(t)$ and $\phi_D(t)$ again denote the jitters on the outputs of the synchronizer and desynchronizer. All of these jitters will be assumed to be defined with respect to an unjittered reference signal and to be positive if their associated signals are ahead of it. In Section III the output of the phase comparator and the jitter on the output of the synchronizer were identical, and we denoted them both by $\phi_S(t)$. When there is input jitter, these two jitters are no longer identical and a new symbol must be introduced for one of them. We have chosen to still call the jitter on the output of the synchronizer $\phi_S(t)$. The symbol $\phi_{SPC}(t)$ will be used for the output of the synchronizer's phase comparator. We have

$$\phi_{SPC}(t) = \phi_S(t) - \phi_I(t).$$

In Appendix B it is shown that with input jitter accounted for the spectrum of waiting time jitter is given by

$$\begin{aligned} S_S(f) &= \operatorname{sinc}^2 f \cdot \hat{Q}(f) + \sum_{n=1}^{\infty} \left(\frac{\rho}{2\pi n}\right)^2 (\delta(f-n) + \delta(f+n)) \\ &\qquad + \operatorname{sinc}^2 f \cdot \operatorname{rep} S_I(f) \\ &\triangleq S_{S,A}(f) + S_{S,B}(f) + S_{S,C}(f), \end{aligned} \tag{6}$$

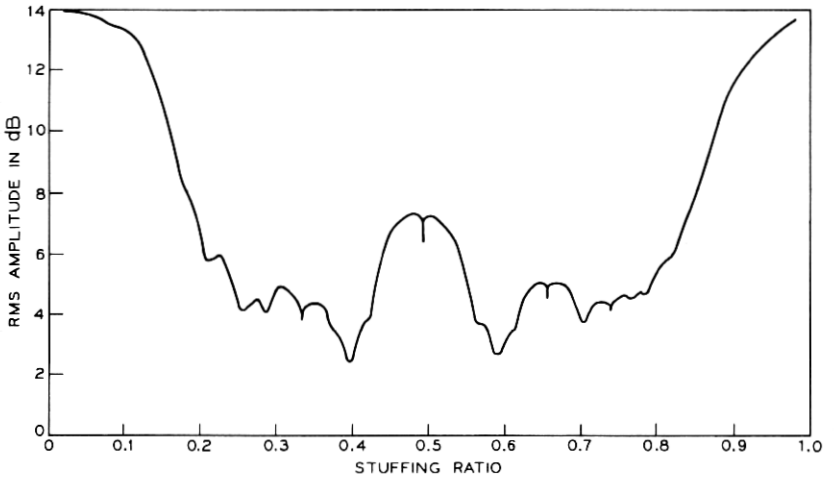

Fig. 11—An experimental graph of the rms amplitude of filtered waiting time jitter as a function of ρ.

where

$$\hat{Q}(f) = \sum_{n=1}^{\infty} \left(\frac{1}{2\pi n}\right)^2 (\text{rep } Z_n(f - n\rho) + \text{rep } Z_n(f + n\rho)) \tag{7}$$

$$Z_n(f) = \mathfrak{F}\{z_n(t)\}$$

$$= \int_{-\infty}^{\infty} z_n(t) e^{-j2\pi ft}\, dt,$$

$$z_n(t) = E\{\exp\{-j2\pi n(\phi_I(t) - \phi_I(0))\}\},$$

$S_I(f)$ is the spectrum of the input jitter, and E denotes expectation.

The input jitter $\phi_I(t)$ will usually only have significant power in frequencies that are quite small in comparison to 1 cycle per stuffing opportunity. When this is the case, the approximation (see Figure 12)

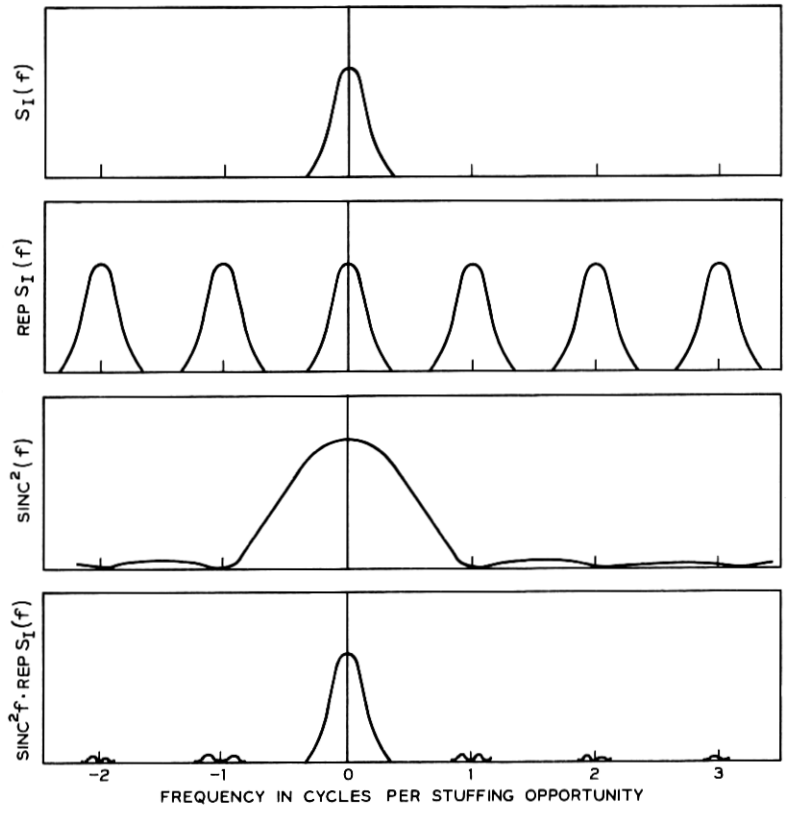

Fig. 12—Approximating $\text{sinc}^2 f \cdot \text{rep } S_I(f)$ by $S_I(f)$.

$$\begin{aligned}\operatorname{sinc}^2 f \cdot \operatorname{rep} S_I(f) &\doteq \operatorname{sinc}^2 f \cdot S_I(f) \\ &\doteq S_I(f)\end{aligned}$$

can be used to simplify (6) to

$$S_S(f) \doteq \operatorname{sinc}^2 f \cdot \hat{Q}(f) + \sum_{n=1}^{\infty} \left(\frac{\rho}{2\pi n}\right)^2 (\delta(f-n) + \delta(f+n)) + S_I(f). \quad (8)$$

The input jitter makes its presence felt in two ways. The first way is simply in the appearance of the feedthrough term $S_I(f)$ (or, more precisely, $\operatorname{sinc}^2 f \cdot \operatorname{rep} S_I(f)$). The second way is in the smearing of spectral lines. The function $\hat{Q}(f)$ has the same functional form as $Q(f)$, but the envelope functions $Z_n(f)$ replace impulses.

The envelope functions $Z_n(f)$ are difficult to compute in general. Evaluating them requires evaluating the same type expressions that must be evaluated to find the spectrum of exponentially modulated carriers. This latter problem has been a traditionally difficult one. Exact evaluations for the special cases of Gaussian input jitter and sinusoidal input jitter and approximate evaluations for small amplitude input jitter are possible.

5.1.1 *Gaussian Input Jitter*

If $\phi_I(t)$ is Gaussian with zero mean and covariance $C_I(t)$, then the random variable $\phi_I(t) - \phi_I(0)$ is Gaussian with zero mean and covariance $2(C_I(0) - C_I(t))$. By the well known formula for the characteristic function of a Gaussian random variable,

$$\begin{aligned}z_n(t) &= E\{\exp\{-j2\pi n(\phi_I(t) - \phi_I(0))\}\} \\ &= \exp\{-(2\pi n)^2(C_I(0) - C_I(t))\}.\end{aligned}$$

Using the infinite series expansion for the exponential function, we have

$$\begin{aligned}z_n(t) &= \exp\{-(2\pi n)^2 C_I(0)\} \exp\{(2\pi n)^2 C_I(t)\} \\ &= \exp\{-(2\pi n)^2 C_I(0)\} \sum_{k=0}^{\infty} \frac{(2\pi n)^{2k}}{k!} C_I^k(t).\end{aligned}$$

Therefore,

$$\begin{aligned}Z_n(f) &= \mathfrak{F}\{z_n(t)\} \\ &= \exp\{-(2\pi n)^2 C_I(0)\} \sum_{k=0}^{\infty} \frac{(2\pi n)^{2k}}{k!} \mathfrak{F}\{C_I^k(t)\}. \\ &= \exp\{-(2\pi n)^2 C_I(0)\} \delta(f) \\ &\quad + \exp\{-(2\pi n)^2 C_I(0)\} \sum_{k=1}^{\infty} \frac{(2\pi n)^{2k}}{k!} \underbrace{S_I(f) * \cdots * S_I(f)}_{k \text{ terms}}. \quad (9)\end{aligned}$$

The envelope $Z_n(f)$ is composed of an impulse at the origin (the carrier line in exponential modulation theory) and an infinite sum of kth order convolutions of the input jitter spectrum with itself.

5.1.2 *Sinusoidal Input Jitter*

If the input jitter is sinusoidal, exact results are also possible. Sinusoidal input jitter can be modeled by the random process

$$\phi_I(t) = \beta \sin (2\pi Ft + \theta),$$

where β and F are constants and θ is a random variable distributed uniformly on $[0, 2\pi)$. [Introducing θ is necessary to randomize the epoch and make $\phi_I(\cdot)$ stationary.]

By direct substitution,

$$\begin{aligned} z_n(t) &= E\{\exp\{-j2\pi n(\phi_I(t) - \phi_I(0))\}\} \\ &= E\{\exp\{-j2\pi n\beta \sin (2\pi Ft + \theta)\} \exp\{j2\pi n\beta \sin \theta\}\} \\ &= E\{\exp\{j2\pi n\beta \sin (-2\pi Ft - \theta)\} \exp\{j2\pi n\beta \sin \theta\}\}. \end{aligned}$$

Using the expansion

$$e^{j\lambda \sin x} = \sum_{k=-\infty}^{\infty} J_k(\lambda) e^{jkx},$$

where the $J_k(\lambda)$ are Bessel functions of the first kind (see, for example, equation 7.53 of Ref. 12) in this equation, we have

$$\begin{aligned} z_n(t) &= E\left\{\sum_{k=-\infty}^{\infty} J_k(2\pi n\beta) e^{-jk(2\pi Ft+\theta)} \cdot \sum_{l=-\infty}^{\infty} J_l(2\pi n\beta) e^{jl\theta}\right\} \\ &= \sum_{k,l=-\infty}^{\infty} J_k(2\pi n\beta) J_l(2\pi n\beta) e^{-jk2\pi Ft} E\{e^{j(l-k)\theta}\} \\ &= \sum_{k=-\infty}^{\infty} J_k^2(2\pi n\beta) e^{-jk2\pi Ft}. \end{aligned}$$

Therefore,

$$Z_n(f) = \sum_{k=-\infty}^{\infty} J_k^2(2\pi n\beta)\ \delta(f + kF). \tag{10}$$

The transform $Z_n(f)$ consists of a string of impulses stretching from $-\infty$ to $+\infty$ and separated from each other by F cycles per stuffing opportunity.

5.1.3 *Small Signal Approximations*

Small signal approximations for the $Z_n(f)$ can be derived easily using the power series expansion for an exponential function. We have

$$\begin{aligned} z_n(t) &= E\{\exp\{-j2\pi n(\phi_I(t) - \phi_I(0))\}\} \\ &= 1 - j2\pi n E\{\phi_I(t) - \phi_I(0)\} \\ &\quad + \frac{1}{2!}(-j2\pi n)^2 E\{(\phi_I(t) - \phi_I(0))^2\} + \cdots \\ &= 1 - \tfrac{1}{2}(2\pi n)^2 E\{(\phi_I(t) - \phi_I(0))^2\} + \cdots \\ &= 1 - (2\pi n)^2(C_I(0) - C_I(t)) + \cdots, \end{aligned}$$

and

$$\begin{aligned} Z_n(f) &= \mathfrak{F}[z_n(t)] \\ &= \delta(f) - (2\pi n)^2(C_I(0)\,\delta(f) - S_I(f)) + \cdots. \end{aligned} \tag{11}$$

If n and the input jitter are small enough, it will be reasonable to approximate $Z_n(f)$ by the first few terms of this expansion.

The simplest such approximation is

$$Z_n(f) \doteq \delta(f). \tag{12}$$

Taking one more term gives the better approximation

$$\begin{aligned} Z_n(f) &\doteq \delta(f) - (2\pi n)^2(C_I(0)\,\delta(f) - S_I(f)) \\ &= (1 - (2\pi n)^2 C_I(0))\,\delta(f) + (2\pi n)^2 S_I(f). \end{aligned} \tag{13}$$

Both of these approximations have the desirable property of preserving total power.

The power in the term $(2\pi n)^2 S_I(f)$ can be used as a guide for determining which of these approximations (if either) is reasonable. For all n, the total power in $Z_n(f)$ is 1. If

$$(2\pi n)^2 \int_{-\infty}^{\infty} S_I(f)\,df \triangleq (2\pi n)^2 P_I$$

is very small in comparison to one (say < 0.01), the approximation

$$Z_n(f) \doteq \delta(f)$$

will be adequate. For moderate power (say $0.01 < (2\pi n)^2 P_I < 0.1$), the second approximation will still be reasonable.

For a given input jitter power, either of these approximations is better for small n than large. For weak input jitter

$$Z_n(f) \doteq \delta(f)$$

will be reasonable for small n, but not for large. Thus, the effect of weak input jitter is to smear the high order n-lines. [The feedthrough

term will be negligible because if $Z_n(f) \doteq \delta(f)$ is reasonable for even small n, $\text{sinc}^2 f \cdot \text{rep } S_I(f)$ will be negligible in comparison to $\text{sinc}^2 f \cdot \hat{Q}(f)$].

5.2 *Filtered Waiting Time Jitter Power with Gaussian Input Jitter*

When the effect of input jitter is considered, the power in filtered waiting time jitter is again given by

$$P_D(\rho) = \int_{-\infty}^{\infty} |H(f)|^2 S_S(f)\, df,$$

but with $S_S(f)$ as defined by equation (6). Let $P_{D,A}(\rho)$, $P_{D,B}(\rho)$, and $P_{D,C}$ denote the components of $P_D(\rho)$ due to $S_{S,A}(f)$, $S_{S,B}(f)$, and $S_{S,C}(f)$ respectively. The power $P_{D,C}$ is a constant independent of ρ. If

$$\text{sinc}^2 f \cdot \text{rep } S_I(f) \doteq S_I(f),$$

then

$$P_{D,C} \doteq \int_{-\infty}^{\infty} |H(f)|^2 S_I(f)\, df,$$

which is the power of the jitter that would be present at the output of the syndes (synchronizer-desynchronizer pair) if its only effect were to filter the input jitter. The jitter power added to the bit stream by pulse stuffing is to within this approximation

$$\Delta P_D(\rho) = P_{D,A}(\rho) + P_{D,B}(\rho).$$

Computer-drawn graphs of $\Delta P_D(\rho)$ for Gaussian input jitter appear in Figures 13 through 16. The transfer function $H(f)$ was assumed to equal that of Figure 9 for Figures 13 and 15 and that of Figure 10 for Figures 14 and 16. For Figures 13 and 14

$$S_I(f) = \frac{1}{2\pi}\left(\frac{1}{10}\right)^2 \frac{0.2}{(0.1)^2 + f^2},$$

and for Figures 15 and 16

$$S_I(f) = \frac{1}{2\pi}\left(\frac{1}{4}\right)^2 \frac{0.2}{(0.1)^2 + f^2}.$$

Both of these spectra are RC with a cutoff at 0.1 cycle per stuffing opportunity. The rms amplitude of the jitter of the first is 1/10 slot, and of the second, 1/4 slot. The first jitter spectrum is felt to be representative of what will typically be encountered in the field.

A comparison of Figures 9, 13, and 15 and of Figures 10, 14, and 16 shows that the effect of input jitter is to erode the peaks and valleys

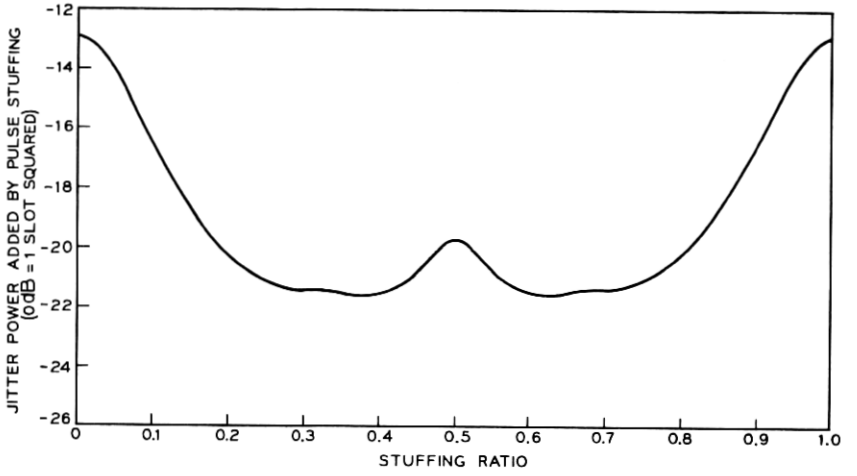

Fig. 13—A theoretical graph of the jitter power added by pulse stuffing as a function of ρ. The jitter on the input to the syndes is assumed to be Gaussian with an rms amplitude of 1/10 slot and an RC spectrum with a corner frequency of 0.1 cycle per stuffing opportunity. The transfer function $H(f)$ is assumed to have a double pole at 0.12 cycle per stuffing opportunity.

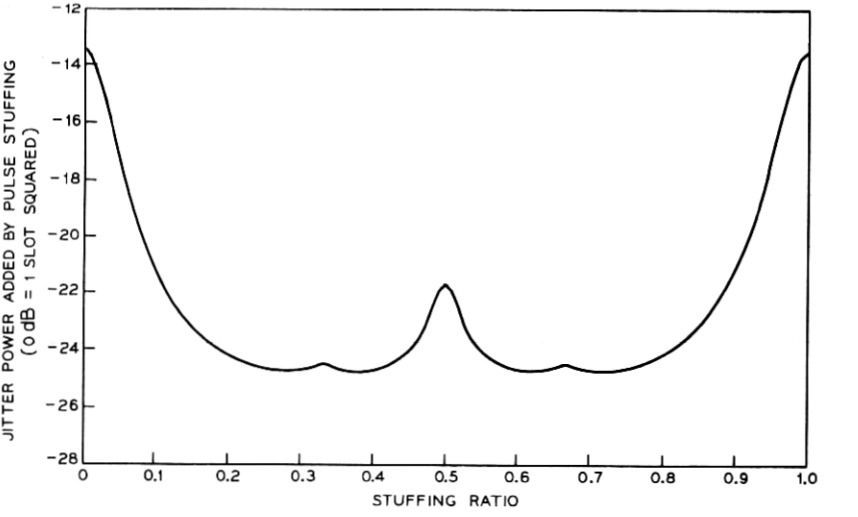

Fig. 14—A theoretical graph of the jitter power added by pulse stuffing as a function of ρ. The jitter on the input to the syndes is assumed to be Gaussian with an rms amplitude of 1/10 slot and an RC spectrum with a corner frequency of 0.1 cycle per stuffing opportunity. The transfer function $H(f)$ is assumed to have a double pole at 0.06 cycle per stuffing opportunity.

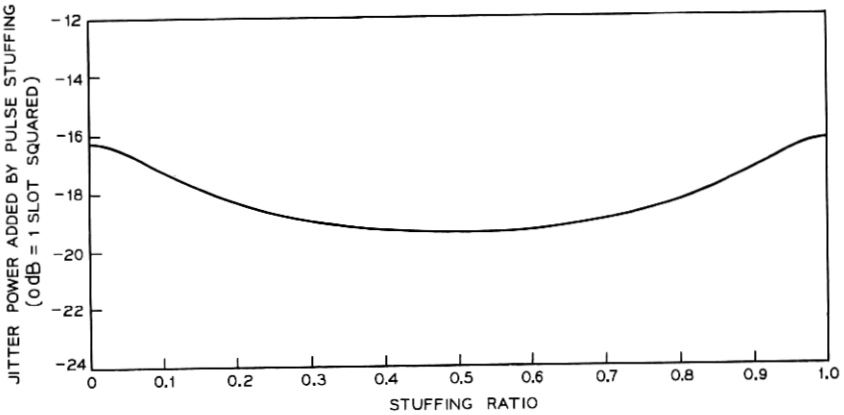

Fig. 15—A theoretical graph of the jitter power added by pulse stuffing as a function of ρ. The jitter on the input to the syndes is assumed to be Gaussian with an rms amplitude of 1/4 slot and an RC spectrum with a corner frequency of 0.1 cycle per stuffing opportunity. The transfer function $H(f)$ is assumed to have a double pole at 0.12 cycle per stuffing opportunity.

of the no input jitter graphs. It is felt that this erosion will occur for almost all input jitter and not just for Gaussian input jitter with a spectrum of the above form. Thus, the choice of ρ is not so critical as it appears to be in Figures 9 and 10 when, as is usually the case, input jitter is not negligible. Notice, however, that even with non-negligible input jitter, there is still an advantage in using a narrow phase-locked loop. The graphs of Figures 14 and 16 are typically 3 dB below those of Figures 13 and 15.

5.3 *A Bound on the Power in Filtered Waiting Time Jitter*

By neglecting the effect of the filter in the desynchronizer, it is possible to obtain a simple bound on the power in filtered waiting time jitter. This bound is quite weak, but will be useful in the next section to bound the accumulation rate of filtered waiting time jitter in chains of syndes.

Let

$$H_{\max} = \max_{f \in (-\infty, \infty)} | H(f) |.$$

Then

$$P_D \leqq H_{\max}^2 P_S$$

where

$$P_S = \int_{-\infty}^{\infty} S_S(f)\, df$$

$$= \int_{-\infty}^{\infty} S_{S,A}(f)\, df + \int_{-\infty}^{\infty} S_{S,B}(f)\, df + \int_{-\infty}^{\infty} S_{S,C}(f)\, df$$

$$\triangleq P_{S,A} + P_{S,A} + P_{S,C} .$$

From equations (32), (31), and (33) of Appendix B

$$P_{S,A} = 1/12,$$

$$P_{S,B} = \rho^2/12 \leqq 1/12,$$

and

$$P_{S,C} = P_I ,$$

where P_I is the input jitter power. Therefore

$$P_D \leqq H_{\max}^2(1/6 + P_I). \tag{14}$$

If there is no peaking,

$$H_{\max} = H(0) = 1$$

and

$$P_D \leqq 1/6 + P_I . \tag{15}$$

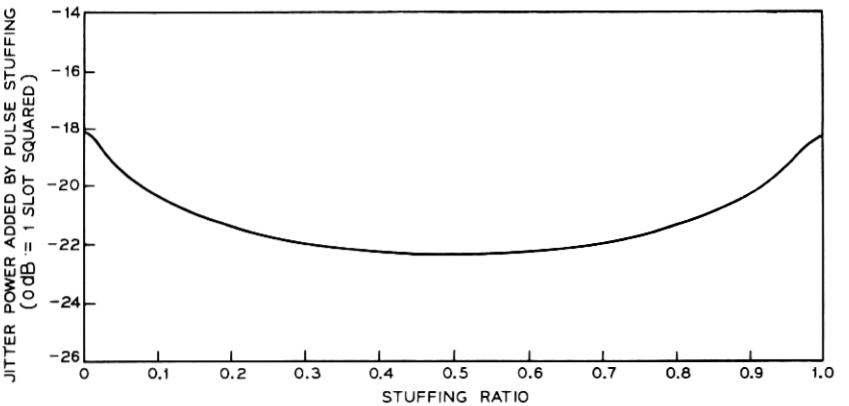

Fig. 16—A theoretical graph of the jitter power added by pulse stuffing as a function of ρ. The jitter on the input to the syndes is assumed to be Gaussian with an rms amplitude of 1/4 slot and an RC spectrum with a corner frequency of 0.1 cycle per stuffing opportunity. The transfer function $H(f)$ is assumed to have a double pole at 0.06 cycle per stuffing opportunity.

VI. WAITING TIME JITTER ACCUMULATION

6.1 *Theoretical Bound*

A question of much engineering interest is how fast filtered waiting time jitter accumulates in tandem connections of syndes. Although the bound (15) is quite weak, it does guarantee that when there is no peaking in any of the transfer functions of the desynchronizers in the chain, the rms amplitude of the jitter on the output of the Nth syndes is no greater than $\sqrt{N}/6$,* and thus that the rate of accumulation of filtered waiting time jitter is no faster than $\sqrt{N}$. Notice that to obtain this bound on the growth rate, it was not necessary to assume the stuffing ratios at each of the synchronizers identical nor the transfer functions of each of the desynchronizers identical.

6.2 *Experimental Data*

The power of the filtered waiting time jitter at the output of a chain of M12 syndes was measured for chain lengths N of 1, 2, 4, 8, and 16 and six different stuffing ratios. The recorded powers are listed in Table IV and plotted in Figure 17.

The upper bound†

$$P_{D,N} \leqq N/6$$

is plotted for comparison in each of the six graphs. The bound is typically about 15 dB above the data. No data are inconsistent with it.

The other line plotted in each of the graphs is

$$P_{D,N} = NP^*_{D,1}\,, \tag{16}$$

where $P^*_{D,1}$ is the theoretical power in filtered waiting time jitter from just one syndes. The values used for $P^*_{D,1}$ were taken from the computer program that produced the graph of Figure 9 and are listed in Table IV for convenience. This line was plotted because it seems to be a reasonable empirical approximation to the data.

The fact that $P_{D,2} < P_{D,1}$ for low stuffing ratios is rather surprising. We do not have a completely satisfactory explanation. For the stuffing ratios where this decrease in power occurs, the 1^--lines and 1^+-lines

---

* It is of course being tacitly assumed here that the input to the first syndes is jitter free and that no other jitters (such as repeater jitter) are being introduced along the chain. A bound including the effects of other jitters could easily be obtained from (15) also.

† There is about 0.15 dB peaking in the phase-locked loop of an M12 so we should strictly be using a bound based on (14) rather than (15). For this slight amount of peaking and the chain lengths considered here, the difference is negligible.

TABLE IV—ACCUMULATION DATA

Stuffing Ratio	Jitter Powers in dB (0 dB = 1 Slot Squared)					
	Theoretical	Experimental				
ρ	N = 1	N = 1	N = 2	N = 4	N = 8	N = 16
0.018	−11.8	−10.9	−13.1	−10.0	− 6.1	− 2.2
0.092	−17.3	−14.8	−20.7	−17.1	− 9.5	− 5.7
0.167	−21.5	−20.7	−18.4	−19.0	−16.8	−10.3
0.241	−22.9	−21.8	−19.6	−16.8	−12.8	− 6.6
0.316	−22.6	−20.5	−15.2	−14.9	−11.7	− 9.1
0.391	−24.5	−20.7	−19.8	−15.6	−12.5	− 9.6

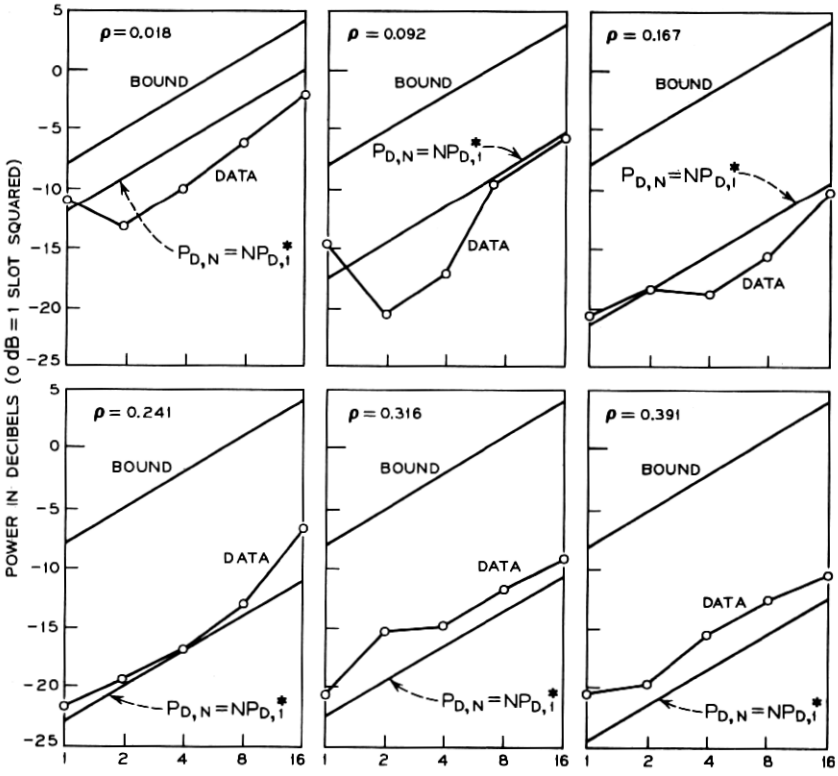

Fig. 17—Experimental accumulation data as a function of log N.

of $\hat{Q}(f)$ are within the passband of $H(f)$. It is felt that an explanation lies partly in the fact that $Z_1(f)$ may (and the approximation of Subsection 5.1.3 suggests it will) throw much of the power in these lines out of the passband of $H(f)$. If this idea is pursued and calculations made, however, it appears that while this phenomenon helps, it cannot be solely responsible. Multiple stuffing may possibly have played a role here also.

VII. SUMMARY

Expressions giving the spectrum of waiting time jitter both when there is and is not significant input jitter have been found. Using these theoretical expressions, graphs of the jitter power added by pulse stuffing versus the stuffing ratio have been drawn. These graphs indicate that when there is no input jitter there is much to be gained by intelligently choosing the stuffing ratio, but that with a typical amount of input jitter present, much of the advantage is lost.

Bounds on the power in filtered waiting time jitter have been found, and it has been shown that when there is no peaking in the desynchronizers of a chain of syndes, the rms amplitude of filtered waiting time jitter accumulates at a rate no faster than the square root of the number of syndes in the chain.

VIII. ACKNOWLEDGMENTS

This paper could not have been written without the assistance of M. R. Aaron, who introduced the author to the waiting time jitter problem, assembled a collection of waiting time jitter references, and contributed greatly through informal discussions. He was the first to notice the applicability of the work of J. E. Iwerson to the waiting time jitter problem. In addition the author is grateful to the M12 multiplex group for assisting in making the laboratory measurements. In particular, A. A. Geigel was most helpful in explaining the operation and circuitry of the M12 multiplex and in collecting the test equipment needed.

APPENDIX A

In this appendix the spectrum $S_s(f)$ of $\phi_s(t)$ is calculated. As noted previously, the procedure used will be to (*i*) write an equation describing waiting time jitter waveforms, (*ii*) introduce initial condition random variables into this equation in such a way that a stationary ensemble

of waiting time jitter waveforms is defined, (*iii*) compute the covariance of the waiting time jitter random process, and (*iv*) Fourier transform this covariance to obtain the power spectrum.

Let $[\cdot]$ denote the greatest integer function, that is, let

$$[x] = \begin{cases} \vdots & \vdots \\ -1, & -1 \leqq x < 0 \\ 0, & 0 \leqq x < 1. \\ 1, & 1 \leqq x < 2 \\ \vdots & \vdots \end{cases}$$

In Figure 18 a waiting time jitter waveform is drawn assuming stuffing opportunities occur at integer times and that just after stuffing at time $t = 0$, $\phi_S(\cdot)$ equals $\Lambda - 1$. With the aid of the greatest integer function an equation describing the waveform of Figure 18 can be written. It is

$$\phi_S(t) = (\Lambda - 1) + \rho t - [\rho[t]]. \tag{17}$$

Obtaining this equation is the key step in finding the spectrum of waiting time jitter. The constant term $\Lambda - 1$ is needed to make $\phi_S(0) = \Lambda - 1$. The second term ρt generates the linearly increasing portion of the waveform $\phi_S(t)$. Stuffs are made by $[\rho[t]]$. The reader should convince himself that this nesting of greatest integer functions puts stuffs in the proper locations.

Equation (17) defines $\phi_S(\cdot)$ at a stuffing time to be equal to its value just after a stuff has been made if one is to be made. In other words, it makes the function $\phi_S(\cdot)$ continuous from the right. This convention

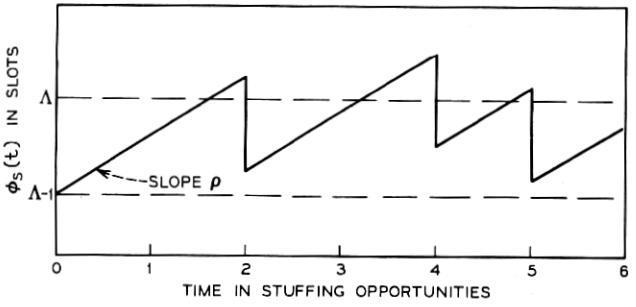

Fig. 18—A waiting time jitter waveform starting at $\Lambda - 1$ at time $t = 0$.

is as good as any. For the purposes here it makes little difference how $\phi_S(\cdot)$ is defined at switching times.

A waiting time jitter waveform drawn at random from a stationary ensemble of waiting time jitter waveforms (see Figure 19) will not in general (in fact almost surely will not) have stuffing opportunities coming at integer times. Define the random variable τ as how long before time $t = 0$ a stuffing opportunity last occurred. Over the ensemble τ will be distributed uniformly on the interval [0, 1).

Define the random variable ζ as by how much $\phi_S(\cdot)$ exceeded $\Lambda - 1$ at time $t = -\tau^+$ (see Figure 19). The random variable ζ must exist in the interval [0, 1). It cannot be less than 0 because $\phi_S(\cdot)$ never is less than $(\Lambda - 1)$. It must be less than 1 because if $\phi_S(\cdot)$ exceeds Λ just before the stuffing opportunity at time $t = -\tau$, a stuff will be

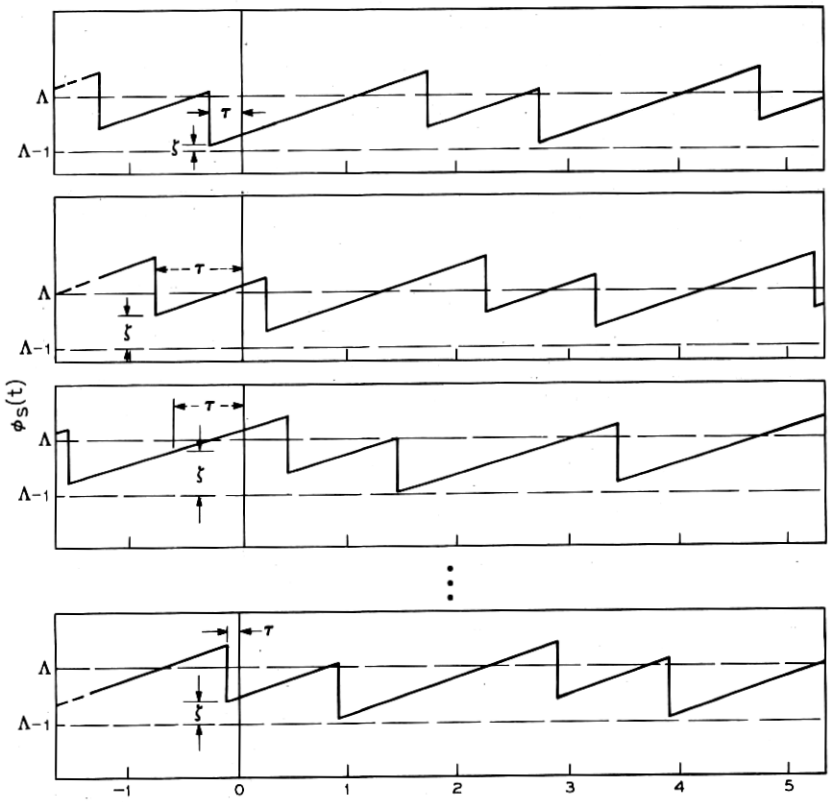

Fig. 19—An ensemble of waiting time jitter waveforms.

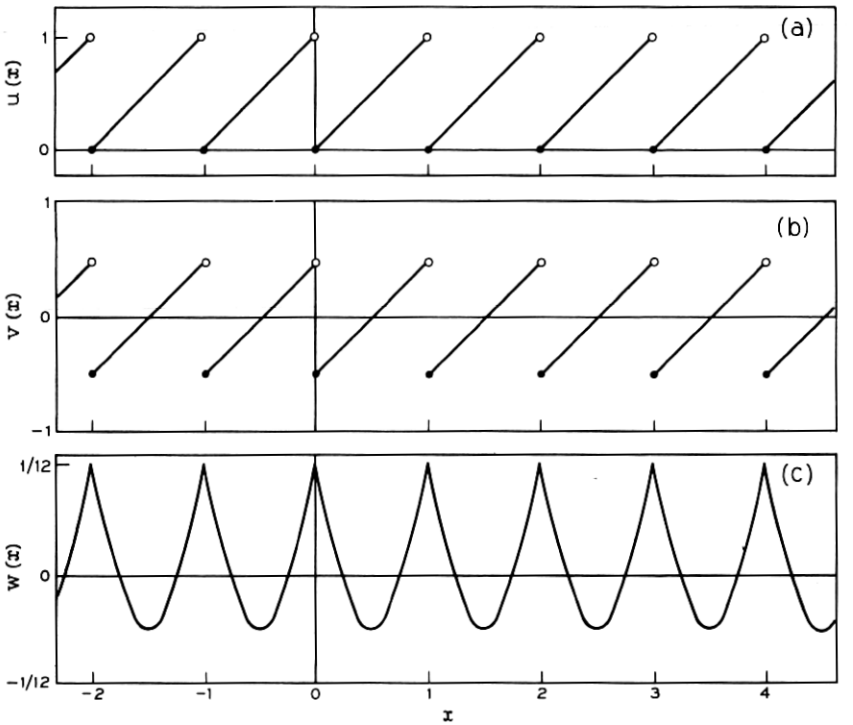

Fig. 20—Graphs of the functions $u(x)$, $v(x)$, and $w(x)$.

made. Over the stationary ensemble, ζ will be independent of τ and distributed uniformly over [0, 1).

A modified version of equation (17) that allows for nonzero ζ and τ is

$$\phi_S(t) = (\Lambda - 1) + \zeta + \rho(t + \tau) - [\zeta + \rho[t + \tau]]. \tag{18}$$

Define (see Figure 20a)

$$\begin{aligned} u(x) &= x - [x] \\ &= x \bmod 1. \end{aligned}$$

An equation equivalent to (18) is

$$\phi_S(t) = (\Lambda - 1) + u(\zeta + \rho[t + \tau]) + \rho u(t + \tau). \tag{19}$$

The next step in the procedure is to find the covariance of the random process $\phi_S(\cdot)$. By definition the covariance $C_S(t)$ of $\phi_S(\cdot)$ is given by

$$C_S(t) = E\{(\phi_S(s + t) - \mu_S)(\phi_S(s) - \mu_S)\},$$

where

$$\mu_S = E\{\phi_S(t)\}$$

and E denotes expectation.

The mean μ_S is not difficult to evaluate. We have

$$\begin{aligned}\mu_S &= E\{\phi_S(0)\}\\ &= E\{(\Lambda - 1) + u(\zeta + \rho[\tau]) + \rho u(\tau)\}\\ &= E\{(\Lambda - 1) + u(\zeta) + \rho u(\tau)\}\\ &= \Lambda - 1 + 1/2 + \rho/2.\end{aligned}$$

Define (see Figure 20b)

$$v(x) = u(x) - 1/2.$$

Then, for all t

$$\phi_S(t) - \mu_S = v(\zeta + \rho[t + \tau]) + \rho v(t + \tau). \tag{20}$$

Returning to the evaluation of $C_S(t)$, we have

$$\begin{aligned}C_S(t) &= E\{(\phi_S(t) - \mu_S)(\phi_S(0) - \mu_S)\}\\ &= E\{v(\zeta + \rho[t + \tau])v(\zeta + \rho[\tau])\} + E\{v(\zeta + \rho[t + \tau])\rho v(\tau)\}\\ &\quad + E\{\rho v(t + \tau)v(\zeta + \rho[\tau])\} + E\{\rho v(t + \tau)\rho v(\tau)\}\\ &= E\{v(\zeta + \rho[t + \tau])v(\zeta)\} + E\{v(\zeta + \rho[t + \tau])\rho v(\tau)\}\\ &\quad + E\{\rho v(t + \tau)v(\zeta)\} + E\{\rho v(t + \tau)\rho v(\tau)\}.\end{aligned}$$

The second and third terms in this expansion (cross covariances) are zero. Indeed,

$$\begin{aligned}E\{v(\zeta + \rho[t + \tau])\rho v(\tau)\} &= \rho E\{E\{v(\zeta + \rho[t + \tau])v(\tau) \mid \tau\}\}\\ &= \rho E\{v(\tau)E\{v(\zeta + \rho[t + \tau]) \mid \tau\}\}\\ &= \rho E\{v(\tau)\cdot 0\}\\ &= 0\end{aligned}$$

and

$$\begin{aligned}E\{\rho v(t + \tau)v(\zeta)\} &= \rho E\{E\{v(t + \tau)v(\zeta) \mid \tau\}\}\\ &= \rho E\{v(t + \tau)E\{v(\zeta) \mid \tau\}\}\\ &= \rho E\{v(t + \tau)E\{v(\zeta)\}\}\\ &= E\{v(t + \tau)\cdot 0\}\\ &= 0.\end{aligned}$$

The fact that

$$E\{v(\zeta + \rho[t + \tau]) \mid \tau\} = 0$$

follows once it is observed that $v(\cdot)$ is periodic with period 1 and that the integral of $v(\cdot)$ over any unit length interval is zero. Therefore,

$$C_S(t) = C_{S,A}(t) + C_{S,B}(t),$$

where

$$C_{S,A}(t) = E\{v(\zeta + \rho[t + \tau])v(\zeta)\}$$

and

$$C_{S,B}(t) = \rho^2 E\{v(t + \tau)v(\tau)\}.$$

The covariance $C_{S,B}(t)$ is the easier to evaluate. We have

$$\begin{aligned}
\rho^{-2}C_{S,B}(t) &= E\{v(t + \tau)v(\tau)\} \\
&= \int_0^1 v(t + \tau)v(\tau)\, d\tau \\
&= \int_0^1 v(t + \tau)(\tau - 1/2)\, d\tau \\
&= \int_0^{1-u(t)} (v(t) + \tau)(\tau - 1/2)\, d\tau \\
&\quad + \int_{1-u(t)}^1 (v(t) + \tau - 1)(\tau - 1/2)\, d\tau \\
&= \int_0^1 (v(t) + \tau)(\tau - 1/2)\, d\tau - \int_{1-u(t)}^1 (\tau - 1/2)\, d\tau \\
&= \int_0^1 \tau(\tau - 1/2)\, d\tau - \int_{1-u(t)}^1 (\tau - 1/2)\, d\tau \\
&= 1/12 - (1/2)u(t)(1 - u(t)).
\end{aligned}$$

Define

$$w(t) = 1/12 - (1/2)u(t)(1 - u(t)).$$

Then,

$$C_{S,B}(t) = \rho^2 w(t). \tag{21}$$

A graph of $w(t)$ appears in Figure 20c.

Turning to the calculation of $C_{S,A}(t)$, we have

$$\begin{aligned}
C_{S,A}(t) &= E\{v(\zeta + \rho[t + \tau])v(\zeta)\} \\
&= E\{E\{v(\zeta + \rho[t + \tau])v(\zeta) \mid \tau\}\}.
\end{aligned}$$

The same manipulations that were used to find an expression for $C_{S,B}(t)$ show

$$E\{v(\zeta + \rho[t + \tau])v(\zeta) \mid \tau\} = w(\rho[t + \tau]).$$

Therefore,

$$\begin{aligned} C_{S,A}(t) &= E\{w(\rho[t + \tau])\} \\ &= \int_0^1 w(\rho[t + \tau]\, d\tau \\ &= \int_0^{1-u(t)} w(\rho[t])\, d\tau + \int_{1-u(t)}^1 w(\rho[t + 1])\, d\tau \\ &= (1 - u(t))w(\rho[t]) + u(t)w(\rho[t + 1]). \end{aligned} \tag{22}$$

A typical graph of $C_{S,A}(t)$ is shown in Figure 21.

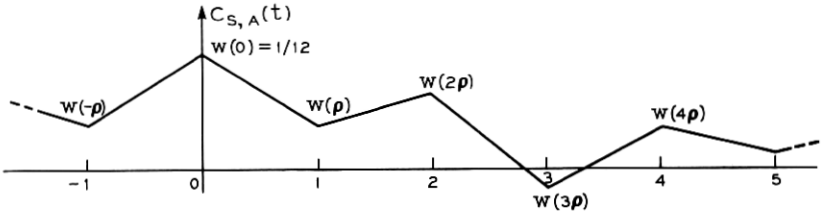

Fig. 21—The covariance $C_{S,A}(t)$.

It is convenient before calculating $S_S(f)$ to mention an equivalent formula for $C_{S,A}(t)$. Define

$$A(t) = \begin{cases} 1 - |t|, & |t| \leqq 1 \\ 0, & |t| > 1 \end{cases}.$$

Then (see Figure 21),

$$C_{S,A}(t) = \sum_{n=-\infty}^{\infty} w(\rho n)A(t - n) \tag{23}$$

$$= A(t) * (w(\rho t) \cdot \text{rep } \delta(t)) \tag{24}$$

where $*$ denotes convolution and for any function $X(f)$

$$\text{rep } X(f) = \sum_{k=-\infty}^{\infty} X(f - k).$$

The Fourier transform of $C_S(t)$ is the spectrum of $\phi_S(t)$. As a matter

of definition

$$\begin{aligned} S_S(f) &= \mathfrak{F}\{C_S(t)\} \\ &= \mathfrak{F}\{C_{S,A}(t)\} + \mathfrak{F}\{C_{S,B}(t)\} \\ &= S_{S,A}(f) + S_{S,B}(f). \end{aligned}$$

The transform $S_{S,B}(f)$ is the easier to take. The function $w(\cdot)$ is periodic with period 1 and has zero mean. Thus, it has the Fourier series expansion

$$w(x) = \sum_{\substack{n=-\infty \\ n\neq 0}}^{\infty} c_n e^{j2\pi nx}$$

where for $n = \pm 1, \pm 2, \cdots$

$$\begin{aligned} c_n &= \int_0^1 w(x)e^{-j2\pi nx}\,dx \\ &= \int_0^1 (1/12 - (1/2)u(x)(1 - u(x)))e^{-j2\pi nx}\,dx \\ &= -(1/2)\int_0^1 u(x)(1 - u(x))e^{-j2\pi nx}\,dx \\ &= -(1/2)\int_0^1 x(1 - x)e^{-j2\pi nx}\,dx \\ &= (2\pi n)^{-2}. \end{aligned}$$

Therefore,

$$\begin{aligned} S_{S,B}(f) &= \mathfrak{F}\{C_{S,B}(t)\} \\ &= \mathfrak{F}\{\rho^2 w(t)\} \\ &= \mathfrak{F}\left\{\rho^2 \sum_{\substack{n=-\infty \\ n\neq 0}}^{\infty} \left(\frac{1}{2\pi n}\right)^2 e^{j2\pi nt}\right\} \\ &= \rho^2 \sum_{\substack{n=-\infty \\ n\neq 0}}^{\infty} \left(\frac{1}{2\pi n}\right)^2 \mathfrak{F}\{e^{j2\pi nt}\} \\ &= \rho^2 \sum_{\substack{n=-\infty \\ n\neq 0}}^{\infty} \left(\frac{1}{2\pi n}\right)^2 \delta(f - n) \\ &= \rho^2 \sum_{n=1}^{\infty} \left(\frac{1}{2\pi n}\right)^2 (\delta(f - n) + \delta(f + n)). \end{aligned} \tag{25}$$

$S_{S,A}(f)$ is only slightly more difficult to compute. Using equation (24) for $C_{S,A}(t)$, we have

$$\begin{aligned} S_{S,A}(f) &= \mathfrak{F}\{C_{S,A}(t)\} \\ &= \mathfrak{F}\{A(t)*(w(\rho t)\cdot \text{rep } \delta(t))\} \\ &= \mathfrak{F}\{A(t)\}\cdot\mathfrak{F}\{w(\rho t)\cdot \text{rep } \delta(t)\} \\ &= \mathfrak{F}\{A(t)\}\cdot(\mathfrak{F}\{w(\rho t)\}*\mathfrak{F}\{\text{rep } \delta(t)\}). \end{aligned}$$

The evaluations

$$\mathfrak{F}\{A(t)\} = \frac{\sin^2 \pi f}{(\pi f)^2} \triangleq \text{sinc}^2 f$$

and

$$\mathfrak{F}\{\text{rep } \delta(t)\} = \text{rep } \delta(f)$$

can be found in most Fourier transform tables. Proceeding as in the evaluation of $S_{S,B}(f)$, we have

$$\begin{aligned} \mathfrak{F}\{w(\rho t)\} &= \mathfrak{F}\left\{\sum_{\substack{n=-\infty \\ n\neq 0}}^{\infty} \left(\frac{1}{2\pi n}\right)^2 e^{j2\pi n\rho t}\right\} \\ &= \sum_{\substack{n=-\infty \\ n\neq 0}}^{\infty} \left(\frac{1}{2\pi n}\right)^2 \mathfrak{F}\{e^{j2\pi n\rho t}\} \\ &= \sum_{\substack{n=-\infty \\ n\neq 0}}^{\infty} \left(\frac{1}{2\pi n}\right)^2 \delta(f - n\rho) \\ &= \sum_{n=1}^{\infty} \left(\frac{1}{2\pi n}\right)^2 (\delta(f - n\rho) + \delta(f + n\rho)). \end{aligned}$$

Assembling these three evaluations, we obtain

$$S_{S,A}(f) = \text{sinc}^2 f\cdot Q(f), \tag{26}$$

where

$$\begin{aligned} Q(f) &= \text{rep } \delta(f)* \sum_{n=1}^{\infty} \left(\frac{1}{2\pi n}\right)^2 (\delta(f - n\rho) + (f + n\rho)) \\ &= \sum_{n=1}^{\infty} \left(\frac{1}{2\pi n}\right)^2 (\text{rep } \delta(f - n\rho) + \text{rep } \delta(f + n\rho)). \end{aligned} \tag{27}$$

APPENDIX B

In this appendix the arguments of the previous appendix are generalized to allow for input jitter. Rather than trying to write an equation

for $\phi_S(t)$ directly, it is easier to first write an equation for $\phi_{SPC}(t)$.

With the jitter sign convention of Section V, the instantaneous frequency of the signal at the input to the synchronizer is $f_0 + \dot{\phi}_I(t)$ and the instantaneous stuffing ratio is $\rho - \dot{\phi}_I(t)$. As in Appendix A, let Λ denote the stuffing threshold, let τ be a random variable denoting how long before time $t = 0$ a stuffing opportunity occurs, and let ζ be a random variable denoting how far above $\Lambda - 1$, $\phi_{SPC}(\cdot)$ was just after the stuffing opportunity at time $t = -\tau$. The random variables ζ and τ will again be independent and distributed uniformly on [0, 1). If there were no stuffing, $\phi_{SPC}(t)$ would evolve as

$$\phi_{SPC}(t) = (\Lambda - 1) + \zeta + \int_{-\tau}^{t} (\rho - \dot{\phi}_I(s))\, ds. \tag{28}$$

In actuality there is stuffing, and at every stuffing opportunity a pulse is stuffed if $\phi_{SPC}(t)$ is greater than Λ at that time. An equation describing $\phi_{SPC}(t)$ when stuffing is taking place is*

$$\begin{aligned}\phi_{SPC}(t) &= (\Lambda - 1) + \zeta + \int_{-\tau}^{t} (\rho - \dot{\phi}_I(s))\, ds \\ &\quad - [\zeta + \int_{-\tau}^{[t+\tau]-\tau} (\rho - \dot{\phi}_I(s))\, ds] \\ &= (\Lambda - 1) + \zeta + \rho(t + \tau) - \phi_I(t) + \phi_I(-\tau) \\ &\quad - [\zeta + \rho[t + \tau] - \phi_I([t + \tau] - \tau) + \phi_I(-\tau)]. \end{aligned} \tag{29}$$

A more convenient form for (29) can be obtained by again introducing the function $u(\cdot)$. It is

$$\begin{aligned}\Phi_{SPC}(t) &= (\Lambda - 1) + u(\zeta + \rho[t + \tau] + \phi_I(-\tau) - \phi_I([t + \tau] - \tau)) \\ &\quad + \rho u(t + \tau) + \phi_I([t + \tau] - \tau) - \phi_I(t).\end{aligned}$$

Since

$$\phi_S(t) = \phi_{SPC}(t) + \phi_I(t),$$

---

* Actually, this equation stuffs more than one time slot if the waveform $\phi_{SPC}(t)$ immediately before a stuffing opportunity has not only increased to a value above Λ, but is also above $\Lambda + 1$ (see Figure 22). A related problem arises if $\phi_{SPC}(t)$ immediately before stuffing is below $\Lambda - 1$ (see Figure 23). The first situation will not occur if the sum of ρ and the negative of the maximum possible negative change of $\phi_I(t)$ in one time slot is less than 1. The second situation will not occur if ρ minus the maximum possible positive change of $\phi_I(t)$ in one time slot is greater than zero. In other words, the model will not deviate from actuality if ρ is not close to 0 or 1 and $\phi_I(t)$ is a low-frequency jitter. These conditions are reasonable and will be assumed to be met.

we have

$$\phi_S(t) = (\Lambda - 1) + u(\zeta + \rho[t + \tau] - \phi_I([t + \tau] - \tau) + \phi_I(-\tau)) + \rho u(t + \tau) + \phi_I([t + \tau] - \tau).$$

The mean μ_S of $\phi_S(t)$ is not difficult to compute. The integral of $u(x)$ over any unit length interval is $1/2$, and therefore

$$E\{\rho u(t + \tau)\} = \rho/2.$$

Similarly,

$$\begin{aligned} &E\{u(\zeta + \rho[t + \tau] - \phi_I([t + \tau] - \tau) + \phi_I(-\tau))\} \\ &\quad = E\{E\{u(\zeta + \rho[t + \tau] - \phi_I([t + \tau] - \tau) + \phi_I(-\tau)) \mid \tau, \phi_I(\cdot)\}\} \\ &\quad = E\{1/2\} \\ &\quad = 1/2. \end{aligned}$$

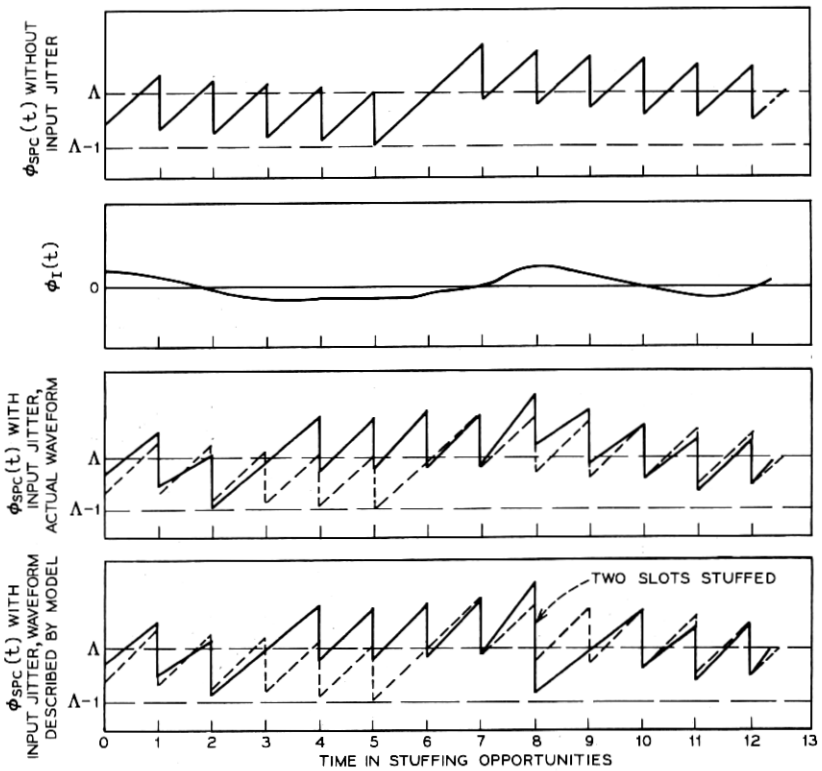

Fig. 22—Deviation of the model from actuality when $\rho = 1^-$.

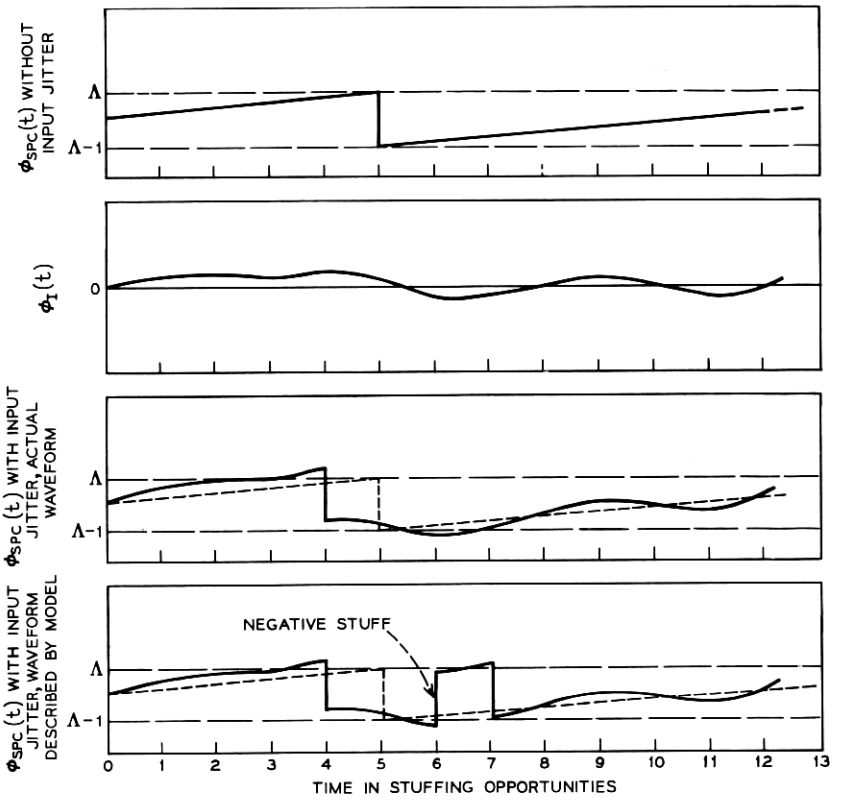

Fig. 23—Deviation of the model from actuality when $\rho = 1^+$.

Therefore,

$$\mu_S = 1/2 + \rho/2$$

and

$$\phi_S(t) - \mu_S = v(\zeta + \rho[t + \tau] - \phi_I([t + \tau] - \tau) + \phi_I(-\tau)) + \rho v(t + \tau) + (\phi_I([t + \tau] - \tau) - \mu_I) \quad (30)$$

where

$$\mu_I = E\{\phi_I(t)\}.$$

The three terms in this equation for $\phi_S(t) - \mu_S$ are easily shown to be uncorrelated. Thus,

$$\begin{aligned} C_S(t) &= E\{(\phi_S(t) - \mu_S)(\phi_S(0) - \mu_S)\} \\ &= E\{v(\zeta + \rho[t + \tau] - \phi_I([t + \tau] - \tau) + \phi_I(-\tau))v(\zeta)\} \\ &\quad + E\{\rho v(t + \tau)\rho v(\tau)]\} \\ &\quad + E\{(\phi_I([t + \tau] - \tau) - \mu_I)(\phi_I(-\tau) - \mu_I)\} \\ &\triangleq C_{S,A}(t) \\ &\quad + C_{S,B}(t) \\ &\quad + C_{S,C}(t). \end{aligned}$$

From Appendix A we have

$$\begin{aligned} C_{S,B}(t) &= E\{\rho^2 v(t + \tau)v(\tau)\} \\ &= \rho^2 w(t) \end{aligned} \tag{31}$$

where

$$w(t) = 1/12 - (1/2)u(t)(1 - u(t)).$$

The evaluation of $C_{S,A}(t)$ is similar to the evaluation of the corresponding term in Appendix A. We have

$$\begin{aligned} &C_{S,A}(t) \\ &= E\{v(\zeta + \rho[t + \tau] - \phi_I([t + \tau] - \tau) + \phi_I(-\tau))v(\zeta)\} \\ &= E\{E\{v(\zeta + \rho[t + \tau] - \phi_I([t + \tau] - \tau) + \phi_I(-\tau))v(\zeta) \mid \tau, \phi_I(\cdot)\}\} \\ &= E\{w(\rho[t + \tau] - \phi_I([t + \tau] - \tau) + \phi_I(-\tau))\}. \end{aligned}$$

Since $\phi_I(t)$ is assumed stationary,

$$\begin{aligned} C_{S,A}(t) &= E\{w(\rho[t + \tau] - \phi_I([t + \tau]) + \phi_I(0))\} \\ &= E\{E\{w(\rho[t + \tau] - \phi_I([t + \tau]) + \phi_I(0)) \mid \phi_I(\cdot)\}\} \\ &= (1 - u(t))E\{w(\rho[t] - \phi_I([t]) + \phi_I(0))\} \\ &\quad + u(t)E\{w(\rho[t + 1] - \phi_I([t + 1]) + \phi_I(0))\} \\ &= A(t)*(r(t)\cdot \text{rep } \delta(t)), \end{aligned} \tag{32}$$

where

$$r(t) = E\{w(\rho t - \phi_I(t) + \phi_I(0))\}.$$

Turning to the final term, we have again using the stationarity of $\phi_I(t)$

$$\begin{aligned} C_{S,C}(t) &= E\{(\phi_I([t+\tau]) - \mu_I)(\phi_I(0) - \mu_I)\} \\ &= E\{E\{(\phi_I([t+\tau]) - \mu_I)(\phi_I(0) - \mu_I) \mid \phi_I(\cdot)\}\} \\ &= (1 - u(t))E\{(\phi_I([t]) - \mu_I)(\phi_I(0) - \mu_I)\} \\ &\quad + u(t)E\{(\phi_I([t+1]) - \mu_I)(\phi_I(0) - \mu_I)\} \\ &= A(t)*(E\{(\phi_I(t) - \mu_I)(\phi_I(0) - \mu_I)\} \cdot \text{rep } \delta(t)) \\ &= A(t)*(C_I(t) \cdot \text{rep } \delta(t)). \end{aligned} \tag{33}$$

The spectrum $S_S(f)$ of the random process $\phi_S(t)$ is the Fourier transform of $C_S(t)$. Let $S_{S,A}(f)$, $S_{S,B}(f)$, and $S_{S,C}(f)$ denote the Fourier transforms of $C_{S,A}(t)$, $C_{S,B}(t)$, and $C_{S,C}(t)$. From Appendix A

$$\begin{aligned} S_{S,B}(t) &= \mathfrak{F}\{C_{S,B}(t)\} \\ &= \sum_{n=1}^{\infty} \left(\frac{\rho}{2\pi n}\right)^2 (\delta(f-n) + \delta(f+n)). \end{aligned} \tag{34}$$

The next easiest Fourier transform to take is that giving $S_{S,C}(f)$. We have

$$\begin{aligned} S_{S,C}(f) &= \mathfrak{F}\{C_{S,C}(t)\} \\ &= \mathfrak{F}\{A(t)*(C_I(t) \cdot \text{rep } \delta(t))\} \\ &= \mathfrak{F}\{A(t)\} \cdot (\mathfrak{F}\{C_I(t)\} * \mathfrak{F}\{\text{rep } \delta(t)\}) \\ &= \text{sinc}^2 f \cdot (S_I(f) * \text{rep } \delta(f)) \\ &= \text{sinc}^2 f \cdot \text{rep } S_I(f). \end{aligned} \tag{35}$$

The evaluation of $S_{S,A}(f)$ is the most difficult. We have

$$\begin{aligned} S_{S,A}(f) &= \mathfrak{F}\{C_{S,A}(t)\} \\ &= \mathfrak{F}\{A(t)*(r(t) \cdot \text{rep } \delta(t))\} \\ &= \mathfrak{F}\{A(t)\} \cdot \mathfrak{F}\{r(t) \cdot \text{rep } \delta(t)\} \\ &= \text{sinc}^2 f \cdot \hat{Q}(f), \end{aligned}$$

where

$$\begin{aligned} \hat{Q}(f) &= \mathfrak{F}\{r(t) \cdot \text{rep } \delta(t)\} \\ &= \mathfrak{F}\{r(t)\} * \text{rep } \delta(f). \end{aligned}$$

The periodic function $w(x)$ has the Fourier series expansion (see Appendix A)

$$w(x) = \sum_{\substack{n=-\infty \\ n=0}}^{\infty} \left(\frac{1}{2\pi n}\right)^2 e^{j2\pi nx}.$$

Therefore,

$$\begin{aligned}
\mathfrak{F}\{r(t)\} &= \sum_{\substack{n=-\infty \\ n\neq 0}}^{\infty} \left(\frac{1}{2\pi n}\right)^2 \mathfrak{F}\{E\{\exp\{j2\pi n(\rho t - \phi_I(t) + \phi_I(0))\}\}\} \\
&= \sum_{\substack{n=-\infty \\ n\neq 0}}^{\infty} \left(\frac{1}{2\pi n}\right)^2 \delta(f - \rho n) * \mathfrak{F}\{E\{\exp\{-j2\pi n(\phi_I(t) - \phi_I(0))\}\}\} \\
&= \sum_{\substack{n=-\infty \\ n\neq 0}}^{\infty} \left(\frac{1}{2\pi n}\right)^2 \delta(f - \rho n) * Z_N(f) \\
&= \sum_{\substack{n=-\infty \\ n\neq 0}}^{\infty} \left(\frac{1}{2\pi n}\right)^2 Z_n(f - \rho n) \qquad (36)
\end{aligned}$$

where

$$Z_n(f) = \mathfrak{F}\{z_n(t)\}$$

and

$$z_n(t) = E\{\exp\{-j2\pi n(\phi_I(t) - \phi_I(0))\}\}.$$

It is convenient to obtain another form for equation (36). Clearly,

$$\begin{aligned}
z_{-n}(t) &= E\{\exp\{-j2\pi(-n)(\phi_I(t) - \phi_I(0))\}\} \\
&= E\{\exp\{-j2\pi n(\phi_I(0) - \phi_I(t))\}\}.
\end{aligned}$$

Since $\phi_I(\cdot)$ is stationary,

$$\begin{aligned}
z_{-n}(t) &= E\{\exp\{-j2\pi n(\phi_I(-t) - \phi_I(0))\}\} \\
&= z_n(-t).
\end{aligned}$$

Therefore,

$$\begin{aligned}
Z_{-n}(f) &\triangleq \mathfrak{F}\{z_{-n}(t)\} \\
&= \int_{-\infty}^{\infty} z_{-n}(t) e^{-j2\pi ft}\, dt \\
&= \int_{-\infty}^{\infty} z_n(-t) e^{-j2\pi ft}\, dt \\
&= \int_{-\infty}^{\infty} z_n(t) e^{-j2\pi(-f)t}\, dt \\
&= Z_n(-f).
\end{aligned}$$

Using this last relation in equation (36), we have

$$\mathfrak{F}\{r(t)\} = \sum_{n=1}^{\infty} \left(\frac{1}{2\pi n}\right)^2 (Z_n(f - \rho n) + Z_{-n}(f + \rho n))$$

$$= \sum_{n=1}^{\infty} \left(\frac{1}{2\pi n}\right)^2 (Z_n(f - \rho n) + Z_n(-f - \rho n)).$$

Therefore,

$$\hat{Q}(f) = \text{rep } \delta(f) * \sum_{n=1}^{\infty} \left(\frac{1}{2\pi n}\right)^2 (Z_n(f - \rho n) + Z_n(-f - \rho n))$$

$$= \sum_{n=1}^{\infty} \left(\frac{1}{2\pi n}\right)^2 (\text{rep } Z_n(f - \rho n) + \text{rep } Z_n(-f - \rho n)). \quad (37)$$

In summary,

$$S_S(f) = \text{sinc}^2 f \cdot \hat{Q}(f)$$

$$+ \sum_{n=1}^{\infty} \left(\frac{\rho}{2\pi n}\right)^2 (\delta(f - n) + \delta(f + n)) + \text{sinc}^2 f \cdot \text{rep } S_I(f) \quad (38)$$

where $\hat{Q}(f)$ is as above.

REFERENCES

1. Mayo, J. S., "Experimental 224 Mb/s PCM Terminals," B.S.T.J., *44*, No. 9, part 2 (November 1965), pp. 1813–1841.
2. Witt, F. J., "An Experimental 224 Mb/s Digital Multiplexer-Demultiplexer Using Pulse Stuffing Synchronization," B.S.T.J., *44*, No. 9, part 2, (November 1965), pp. 1843–1885.
3. Bruce, R. A., "A 1.5 to 6 Megabit Digital Multiplex Employing Pulse Stuffing," IEEE Int. Conf. on Commun., (June 1969), pp. 34–1 to 34–7.
4. Bell Laboratories Staff, *Transmission Systems for Communications*, Western Electric Company, Winston-Salem, North Carolina, 1970.
5. Kozuka, S., "Phase Controlled Oscillator for Pulse Stuffing Synchronization System," Review of the Electrical Communication Laboratory, *17*, Numbers 5-6, (May-June, 1969), pp. 376–387.
6. Matsuura, Y., Kozuka, S., and Yuki, K., "Jitter Characteristics of Pulse Stuffing Synchronization," IEEE Int. Conf. on Commun., (June 1968), pp. 259–264.
7. Iwerson, J. E., "Calculated Quantizing Noise of Single-Integration Delta-Modulation Coders," B.S.T.J., *48*, No. 7, part 3, (September 1969), pp. 2359–2389.
8. Kitamura, Z., K. Terada, and K. Asada, "Asynchronous Logical Delay Line for Elastic Stores," Electronics and Communications in Japan, *50*, (November 1967), pp. 90–99.
9. Bennett, W. R., "Statistics of Regenerative Digital Transmission," B.S.T.J., *37*, No. 6, part 2, (November 1958), pp. 1501–1542.
10. Rowe, H. E., "Timing in a Long Chain of Regenerative Binary Repeaters," B.S.T.J., *37*, No. 6, part 2, (November 1958), pp. 1543–1598.
11. Byrne, C. J., B. J. Karafin, and D. B. Robinson, Jr., "Systematic Jitter in a Chain of Digital Regenerators," B.S.T.J., *42*, No. 6, part 3, (November 1963), pp. 2679–2714.
12. Panter, P. F., *Modulation, Noise, and Spectral Analysis*, New York: McGraw-Hill, 1965.